# NUCLEAR SPIN RELAXATION

# IN THREE SPIN SYSTEMS

A THESIS

Presented to

The Faculty of the Division of Graduate

Studies and Research

by

Ping Pin Yang

In Partial Fulfillment

of the Requirements for the Degree

Doctor of Philosophy

in the School of Chemistry

Georgia Institute of Technology

December, 1971

NUCLEAR SPIN RELAXATION

IN THREE SPIN SYSTEMS

Approved:

Chairman

Date approved by Chairman: Jan. 5, 1972

# ACKNOWLEDGMENTS

The author wishes to thank his advisor, Dr. S. L. Gordon, for his constant guidance through the course of this research. He likes to thank Dr. W. M. Spicer for his arrangement of a research assistantship from the National Science Foundation.

The author is indebted to Dr. T. F. Moran, Dr. R. H. Felton, Dr. H. A. Gersch and Dr. J. O. Williams for their serving on the thesis committee, and to Mr. Gerald O'Brien for his maintenance of the instrumentation. He also wishes to acknowledge and express appreciation to Mrs. Claudine Taylor for her help in typing the thesis.

# TABLE OF CONTENTS

TABLE OF CONTENTS (CONTINUED)

# LIST OF TABLES

## LIST OF FIGURES

## SUMMARY

There are two parts in this thesis. Nuclear magnetic double resonance in chemically exchanging systems is discussed in Part One. Overhauser studies in three spin systems are treated in Part Two.

In Part One, a density matrix description of nuclear magnetic double resonance on chemically exchanging system is developed using a double resonance basis set. The chemical exchange coefficients have many properties analogous to the relaxation coefficients. This allows the density matrix computation to be expressed in terms of symmetric array. The solutions then can be detained in terms of an eigenvalue procedure. The formalism is illustrated by self-exchange in the $AB_2$ system, 2,2,2-trichloroethanol. Comparison of theoretical and experimental double resonance spectra allows the determination of the chemical exchange lifetime and the relaxation parameters.

In Part Two, the simple line approximation of the density matrix equation is used to describe the Overhauser effects in three spin systems. Intramolecular and intermolecular dipolar interactions are studied. The symmetry properties of the relative fractional change of intensities in the weak coupling limit are discussed. In addition, the relations between the relative fractional change of intensities for different double resonance experiments are established. The summation rule for the fractional change and relative fractional change of intensities are found to be very useful. The formalism is illustrated by the ABX system of vinyl bromide.

Two samples of vinyl bromide are investigated. Sample A is degassed. The double resonance experiments indicate 53% intramolecular dipolar interaction. Sample B has a small amount of oxygen added to it. The double resonance experiments indicate 18% intramolecular dipolar interaction.

# PART ONE

## NUCLEAR MAGNETIC DOUBLE RESONANCE IN CHEMICALLY EXCHANGING SYSTEMS

Part One was published in The Journal of Chemical Physics, Volume 54, Number 4, pages 1779 to 1786, 15 February 1971. This article appears as the Appendix of this dissertation and also as reference 1.

# PART TWO

# OVERHAUSER STUDIES IN THREE SPIN SYSTEMS

# CHAPTER I

# INTRODUCTION

Double resonance has been a useful technique for studying the relaxation processes of nuclear spin systems. In this technique, one of the transitions of a high resolution nuclear magnetic resonance spectrum is irradiated by a second radio frequency field and the rest of transitions are observed by a weak rf field. If the strength of the second rf is small so that no splittings are observed, one obtains the well known general Overhauser effect spectra. In this case, the second rf only causes the population changes at various energy levels without affecting the spin energies. If the strength of the second rf is strong, it will produce new transition lines in addition to having the population changes at various levels. Information about the relaxation mechanisms can be obtained from the analysis of double resonance spectra. The single spin system has been studied in great detail by Bloch,[2] Baldeschwieler,[3] Gordon[4] and Rao.[5] Two spin systems 6-9 were investigated extensively, both theoretically and experimentally. $AB_2$[1, 10] and ABX[12] three spin systems were also studied by steady state double resonance.

In general, the double resonance experiments are sensitive to the specific relaxation processes for different kinds of molecules. An advantage of this technique is that information about the relaxation process can be obtained by using only a single set of external conditions.

Weak double resonance experiments, in which the irradiation strength is comparable to the strength of relaxation, are quite sensitive to the relaxation mechanism. In addition, the experiment and spectral analysis of weak double resonance spectra are simpler than those from strong[10] or pulsed[11] double resonance experiments. The absolute relaxation parameters can also be obtained by this method.

Recently, two spin systems were studied by this weak irradiation technique.[6] In this thesis, three spin systems are studied by the same technique.

The density matrix equation and the possible relaxation mechanisms are discussed in Chapter II. The equations for the weak irradiation experiments are formulated in Chapter III. The fractional intensity changes, $F_{ab,cd}$, and relative fractional intensity changes, $G_{ab,cd}$, are defined and discussed in terms of this formulation. Algebraic solutions for the weak coupling limit are given. The computer solution for a tightly coupled three spin system is discussed. The formalism is illustrated by the ABX system vinyl bromide in Chapter IV.

# CHAPTER II

## DENSITY MATRIX FORMALISM FOR DOUBLE RESONANCE

### A. Density Matrix Equation

The spin density matrix equation for double resonance is given by

$$\frac{d\sigma}{dt} = -i[\mathcal{H}_o + \mathcal{H}_1(t) + \mathcal{H}_2(t),\ \sigma] - \Gamma(\sigma - \sigma_o) \tag{1}$$

where $\sigma$ is the spin density matrix, and $\sigma_o$ is $\sigma$ at thermal equilibrium with no rf field. In the high temperature approximation, $\sigma_o = 1/N - q\mathcal{H}_o$, where $q = \hbar/NkT$. Also,

$$\mathcal{H}_o = 2\pi\left\{\sum_i \nu_{oi} I_z(i) + \sum_{i<j} J_{ij} I(i)\cdot I(j)\right\} ,$$

$$\mathcal{H}_1(t) = D_{1+}\ \exp(i\omega_1 t) + D_{1-}\ \exp(-i\omega_1 t) ,$$

$$\mathcal{H}_2(t) = D_{2+}\ \exp(i\omega_2 t) + D_{2-}\ \exp(-i\omega_2 t) ,$$

$$\nu_{oi} = \gamma_i\ \mathcal{H}_0/2\pi,\ D_{2+} = \pi\Sigma\nu_{2i}I_+(i),\ D_{2-} = \pi\Sigma\nu_{2i}I_-(i),$$

$$D_{1+} = \pi\Sigma\nu_{1i}I_+(i)\ ,\ D_{1-} = \pi\Sigma\nu_{1i}I_-(i),\ \nu_{2i} = \frac{\nu_i H_2}{2\pi}\ ,\ \nu_{1i} = \frac{\nu_i H_1}{2\pi}.$$

$\gamma_i$ is the magnetogyric ratio of nucleus i including the chemical shift and $J_{ij}$ is the spin-spin coupling constant between i and j in cycles per second. The $\Gamma(\sigma - \sigma_o)$ term describes relaxation, and is given by

$$\Gamma_{aa'}(\sigma - \sigma_o) = -\sum_{bb'} R_{aa'bb'}(\sigma - \sigma_o)_{bb'} \tag{2}$$

The $R_{aa'bb'}$ matrix elements are given by the Redfield formulation:[16]

$$R_{aa'bb'} = 2J_{aba'b'} - \delta_{a'b'}\sum_c J_{cbca} - \delta_{ab}\sum_c J_{ca'cb'} \tag{3}$$

In equation (3) under extreme narrowing approximation,

$$J_{aba'b'} = \tau_c < <a|\mathcal{H}(t)|b><a'|\mathcal{H}(t)|b'>^* >_{AV} \ldots, \tag{4}$$

where $< \ >_{AV}$ indicates an ensemble average. The summation and symmetry properties of the $R_{aa'bb'}$ are given by equations (6) and (7) in reference 1.

As in reference 1, it is convenient to define a difference matrix $\chi(t)$ by $\chi(t) = \sigma - \sigma_o$. Equation (1) then becomes

$$\frac{d\chi(t)}{dt} = -i[H_o, \chi(t)] - i[\mathcal{H}_2(t), \sigma_o + \chi(t)] - \Gamma(\chi) \tag{5}$$

The calculation for $\chi(t)$ here is based upon the basis set of single resonance, $|a>$, $|b>$ ...etc.,

where
$$\mathcal{H}_o|a> = \omega_a|a>. \tag{6}$$

Small latin letters are used to specify the single resonance basis set. The calculation of $\chi(t)$ in reference 1 is based upon the basis set of double resonance in equation (4) of reference 1. The diagonal elements of $\chi(t)$ calculated here can be interpreted directly as the population changes from the equilibrium spin density matrix.

## B. Relaxation Mechanisms in Three Spin Systems

Three relaxation mechanisms are discussed in this analysis.

### 1. Intramolecular Dipolar Interaction

This is the dipole-dipole interaction between nuclei within the molecule. The interaction Hamiltonian[10] in the laboratory frame is given by

$$\mathcal{H}'(t) = \sum_{q=-2}^{2} \sum_{N} (1)^q H_N^q A_N^{-q} \quad , \tag{7}$$

where

$$A_N^{\pm 2} = I_k^{\pm} S_{k'}^{\pm} \,; \quad A_N^{\pm 1} = \mp \left( I_k^{\pm} S_{k'}^{Z} + I_k^{Z} S_{k'}^{\pm} \right) \;;$$

$$A_N^{o} = \left(\frac{8}{3}\right)^{\frac{1}{2}} \left\{ I_k^Z S_{k'}^Z - \frac{1}{4}\left( I_k^{+} S_{k'}^{-} + I_k^{-} S_{k'}^{-} \right) \right\} \;; \tag{8}$$

and

$$H_N^q = - \left(\frac{6\pi}{5}\right)^{\frac{1}{2}} \hbar \gamma_k \gamma_{k'} r_N^{-3} Y_2^q \left(\theta_N, \Phi_N\right).$$

The subscript N indicates a pair of spins $I_k$ and $S_{k'}$. $r_N$ is the distance between $I_k$ and $S_{k'}$. $Y_2^q(\theta_N, \Phi_N)$ are the spherical harmonics of rank 2 with $\theta_N$ and $\Phi_N$ specifying the orientation of $r_N$ relative to the laboratory coordinate system. The $H_N^q$ are random functions of time. Substituting equation (7) in equation (4) the spectral density becomes

$$J_{aba'b'} = \tau_c \sum_{N \geq N'} \frac{3}{20} \hbar^2 \gamma_{I_N} \gamma_{S_N} \gamma_{I_{N'}} \gamma_{S_{N'}} r_N^{-3} r_{N'}^{-3} \quad x$$

$$(3 \cos^2 \varphi_{NN'} - 1) \sum_q \langle a | A_N^q | b \rangle \langle a' | A_{N'}^q | b' \rangle \tag{9}$$

where $\varphi_{NN'}$ is the angle between $r_N$ and $r_{N'}$. Equation (9) will be written in the following form for convenience in discussing vinyl bromide:

$$J_{\alpha\beta\alpha'\beta'} = \frac{1}{TD} \sum_{N \geq N'} g_{NN'} \sum_q <\alpha|A_N^q|B><\alpha'|A_{N'}^q|B'> \tag{10}$$

where

$$g_{NN'} = \frac{3\cos^2\varphi_{NN'} - 1}{10} \cdot \frac{r_{ab}^6}{r_N^3 r_{N'}^3} \tag{11}$$

and

$$\frac{1}{TD} = \frac{3\gamma^4 \hbar^2 \tau_c}{2\, r_{ab}^6} \tag{12}$$

In vinyl bromide, $r_{ab}$ is the distance between the geminal protons. The dipolar interaction of the geminal protons is the strongest. TD would give the dipolar contribution to the relaxation time of the geminal protons if the vicinal proton were not present.

2. Intermolecular Dipolar Interaction

This is the dipole dipole interaction between nuclei in different molecules. The isotropic external random field is used to describe the intermolecular dipolar interaction, rather than using a detailed sum process.[17] The result of such a model is generally in agreement with experiment. The interaction Hamiltonian for isotropic external random field[10] is given as

$$\mathcal{H}'(t) = \sum_k \gamma_k \left\{ H_k^Z(t) I_k^Z + \tfrac{1}{2}\left[ H_k^+(t) I_k^- + H_k^-(t) I_k^+ \right. \right. \tag{13}$$

where $\quad < |H_k^Z(t)|^2>_{AV} = \tfrac{1}{2} <|H_k^+(t)|^2>_{AV} = \tfrac{1}{2}< |H_k^-(t)|^2>_{AV},$

$$H_k^{\pm}(t) = H_k^X(t) \pm i H_k^Y,$$

$$\text{and } H_k^Z(t),\ H_k^X(t) \text{ and } H_k^Y(t)$$

are the Z, X and Y components of the random field strength respectively at spin site k. For ABX three spin systems, equation (13) can be rewritten as

$$\mathcal{H}'(t) = \sum_{k=A,B,X} \gamma_k \left\{ H_k^Z(t) I_k^Z + \tfrac{1}{2}\left[ H_k^+(t) I_k^- + H_k^-(t) I_k^+ \right] \right\} \tag{14}$$

where A, B and X indicate the nuclear sites A, B and X respectively. From equations (4) and (14), the spectral density can be obtained as

$$\begin{aligned} J_{aba'b'} = \sum_{k=A,B,X} & \frac{\gamma_k^2}{2T_k} \Big\{ <a|I_k^Z|b><a'|I_k^Z|b'> + \\ & \tfrac{1}{2}<|I_k^+|b><a'|I_k^+|b'> + \tfrac{1}{2}<a|I_k^-|b><a'|I_k^-|b'> \Big\} \\ & + \sum_{k<k'} \frac{C_{kk'}\gamma_k\gamma_{k'}(T_k)^{-\frac{1}{2}}(T_{k'})^{-\frac{1}{2}}}{2} \\ & \Big[ <a|I_k^Z|b><a|I_{k'}^Z|b'> + \tfrac{1}{2}<a|I_k^+|b><a'|I_{k'}^+|b'> + \\ & \tfrac{1}{2}<a|I_k^-|b><a'|I_{k'}^-|b'> \Big] \end{aligned} \tag{15}$$

where

$$\frac{1}{T_k} = \frac{2}{3}\gamma_k^2 <|H_k(t)|^2>_{AV} \tau_c, \quad k = A, B, X \tag{16}$$

$$<|H_k(t)|^2>_{AV} = 3 < |H_k^Z(t)|^2>_{AV} = \frac{3}{2} < |H_k^+(t)|^2>_{AV} =$$

$$\frac{3}{2} < |H_k^-(t)|^2 >_{AV}, \; k = A, B, X,$$

and

$$C_{kk'} = \frac{< |H_k^q(t) \, H_{k'}^q(t)| >_{AV}}{\left[ < |H_k^q(t)|^2 >_{AV} < |H_{k'}^q(t)|^2 >_{AV} \right]^{\frac{1}{2}}} \tag{17}$$

$T_k$ is the relaxation time of random field at spin site k. $C_{kk'}$ are the correlation constants between k and k′ varying between 0 to 1 for no correlation and complete correlation.

3. Spin-Rotational Interaction

The interaction between the nuclear spins in a molecule and the magnetic field produced by the rotation of the molecule containing these nuclei is called spin-rotational interaction. The interaction Hamiltonian[18] is given by

$$\mathcal{H}'(t) = \underset{\sim}{I} \cdot \underset{\sim}{C}(t) \cdot \underset{\sim}{J} \;, \tag{18}$$

where $\underset{\sim}{J}$ is the angular momentum of the molecule containing the nuclear spin $\underset{\sim}{I}$, and $\underset{\approx}{C}$ is the spin-rotation tensor. For a spherical molecule the interaction Hamiltonian[18] in the molecular fixed frame is given as

$$\mathcal{H}'(t)^{(i)} = \sum_{q'=-1}^{1} C_{q'} A^{q'} J^{-q'} \;, \tag{19}$$

where $$A^o = I^Z; \; A^{\pm 1} = \mp \frac{1}{\sqrt{2}} I^{\pm} \;;$$

$$J^o = J^Z; \; J^{\pm 1} = \mp \frac{1}{\sqrt{2}} (J^X \pm iJ^Y) \;;$$

$$C_o = C_{\parallel} = C_Z \text{ and } C_{\pm 1} = -C_{\perp} = C_X = C_Y .$$

Transforming A and J from the molecular fixed frame to the laboratory frame by

$$A^{q'} = \sum_q A^q D^{(1)}_{qq'}(\Omega) \text{ and}$$

$$J^{q'} = \sum_{q'} D^{(1)}_{-q'q''}(\Omega) \quad ,$$

the interaction Hamiltonian in the laboratory frame is given by

$$\mathcal{H}'(t) = \sum_{q,q'q''} (-1)^q A^q C_{q'} D^{(1)*}_{q'q}(\Omega) \; D^{(1)}_{-q'q''}(\Omega) \; J^{q''} \tag{20}$$

where $D^{(1)}_{q'q}(\Omega)$ and $D^{(1)}_{-q'q''}$ are rotational matrices.[19] The spectral density is given by Hubbard as

$$J_{aba'b'} = \frac{NIkT}{9\hbar^2} \sum_q \left\{ \frac{(2C_{\perp} + C_{\parallel})^2 \, 2\tau_1}{\left[1+(\omega_I q \tau_1)^2\right]} + \right.$$

$$\left. \frac{2(C_{\parallel} - C_{\perp})^2 \, 2\tau_{12}}{\left[1+(\omega_I q \tau_{12})^2\right]} \right\} \frac{1}{\left(|q|+1\right)} < a|I^q|b> < b'|I^{-q}|a> \tag{21}$$

where

$\tau_1$ is the characteristic time for the change of components of angular momentum $J^q$; $\tau_2$ is the characteristic time for the molecular reorientation and $\tau_{12}$ is defined as $1/\tau_{12} = 1/\tau_1 + 1/\tau_2$. If $\tau_1 \ll \tau_2$, $\tau_{12} \cong \tau_1$, and equation (24) becomes

$$J_{aba'b'} = \sum_q \frac{NIkT}{3\hbar^2}\left(2C_\perp^2 + C_{||}^2\right) x <a|I^q|b><b'|I^{-q}|a'> \qquad (22)$$

This is equivalent in form to the spectral density of the intermolecular dipolar interaction. Therefore, the relaxation mechanism of spin-rotation is mathematically equivalent to the intermolecular dipolar relaxation mechanism. $R_{aa'bb'}$ can be obtained from equations (3) and (22). This interaction has been studied in a number of molecules. For example, in $NH_3$,[20] the contribution to the relaxation time for spin-rotation at 25°C is about 100 seconds. However, the relaxation time for vinyl bromide is about 20 seconds. Therefore, this interaction will not be important for the experiments discussed in this thesis.

# CHAPTER III

# SOLUTION OF DENSITY MATRIX EQUATION

## A. The Energy Level Diagram of an ABX System

The discussion of this section will be in terms of the ABX spin system, vinyl bromide,

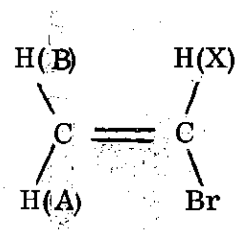


The wave functions, energy values and spectral parameters are given in Chapter IV. The energy level diagram of vinyl bromide is presented as a cube in Figure 1. Each corner in Fig. 1 represents a spin state. The eight spin states are labelled in the weak coupling limit. Each positive sign indicates one spin up and each negative sign indicates one spin down. The order of the signs from left to right is X, B and A, respectively. The top of the energy cube corresponds to the lowest energy. The horizontal ordering of the energy levels assumes $\nu_{oA} > \nu_{oB} > \nu_{oX}$, $J_{AX}$ and $J_{BX}$ are positive and $J_{AB}$ is negative for vinyl bromide.[21] Each edge represents a nondegenerate single quantum transition, each face diagonal connecting 1 or 8 represents a double quantum transition. The other face diagonals represent zero quantum transitions. Double and zero quantum transitions are explicitly indicated for the AB pair in this figure. Each transition has a label

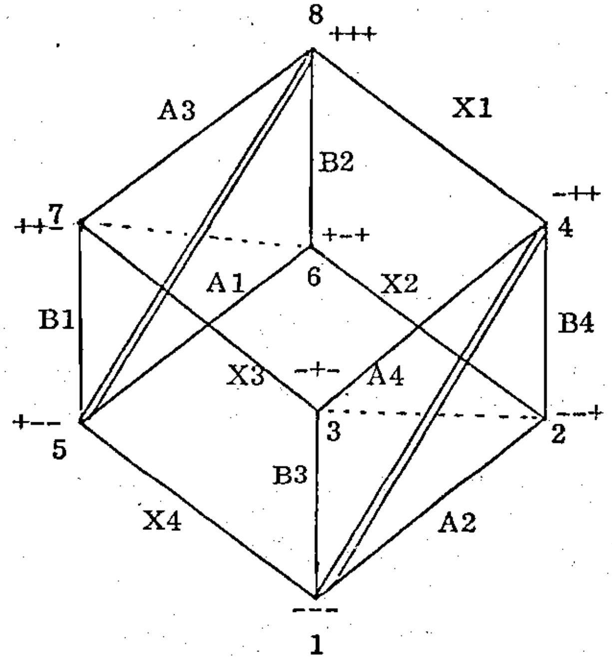


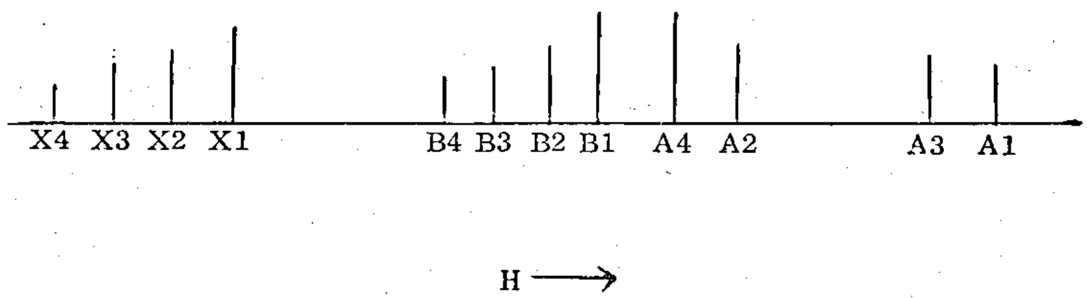


Fig. 1. Energy Level Diagram and Spectrum of ABX System.

shown below:

| | | | | | | | | | | | | |
|---|---|---|---|---|---|---|---|---|---|---|---|---|
| Transition | $5\to 1$ | $6\to 2$ | $7\to 3$ | $8\to 4$ | $4\to 2$ | $3\to 1$ | $8\to 6$ | $7\to 5$ | $4\to 3$ | $2\to 1$ | $8\to 7$ | $6\to 5$ |
| Label | X4 | X3 | X2 | X1 | B4 | B3 | B2 | B1 | A4 | A2 | A3 | A1 |

In the weakly coupled limit, X4, X3, X2 and X1 are X proton transitions; B4, B3, B2 and B1 are B proton transitions; and A4, A2, A3 and A1 are A proton transitions.

When the irradiation strength is weak, it does not produce splittings. Therefore only intensity changes in each line are observed in the double resonance spectra. This is known as the nuclear Overhauser effect.

It is assumed that transition ab is irradiated by a weak rf field. The energy of state b is higher than the energy of state a. If transition ab is well separated from any other line, equation (5) reduces[6] to

$$\sum_c R_{aacc}\,\chi_c = 2I_{2ab} \tag{23}$$

$$\sum_c R_{bbcc}\,\chi_c = -2I_{2ab} \tag{24}$$

and

$$\sum_c R_{c'c'cc}\,\chi_c = 0 \quad c' \neq a, b \tag{25}$$

where $\chi_a = \chi_{aa}, \; \chi_b = \chi_{bb},$

$$I_{2ab} = \frac{q\omega_o}{T_{ab}}\,\Delta_2 \tag{26}$$

$$\Delta_2 = \frac{|d_2|^2 T_2 T_{ab}}{1 + |d_2|^2 T_2 T_{ab} + (\omega_2 - \omega_o)^2 T_2^2} \tag{27}$$

and

$$T_{ab} = T_a - T_b \quad , \tag{28}$$

where $T_a$ and $T_b$ are defined below:

$$\chi_a = T_a I_{ab}, \quad \chi_b = T_b I_{ab} \quad . \tag{29}$$

Then equations (23) to (25) become

$$\sum_c R_{aacc} T_c = 2 \tag{30}$$

$$\sum_c R_{bbcc} T_c = -2 \tag{31}$$

and

$$\sum_c R_{c'c'cc} T_c = 0 \quad c' \neq a, b \quad . \tag{32}$$

$T_c$ interprets the measurements of intensities, the fractional intensity changes are defined by

$$F_{ab,cd} = \frac{I^{DR}_{ab,cd} - I^{SR}_{ab}}{I^{SR}_{ab}} \quad ,$$

where $I_{a'b',ab}$ are the measured intensities. $F_{ab,cd}$[6] can be expressed in terms of the $T_{ab}$'s as F

$$F_{ab,cd} = \frac{T_{ba}}{T_{cd}} \Delta_2 \quad . \tag{34}$$

In equation (34), ab is the line observed and cd is the line irradiated. It is useful to define the relative fractional change of intensity. The relative fractional change of intensity $G_{ab, cd}$, is given by

$$G_{ab, cd} = \frac{F_{ab, cd}}{|F_{cd, cd}|} = \frac{T_{ab}}{|T_{cd}|} \tag{35}$$

where line ab is observed and line cd is irradiated.

The $F_{ab, cd}$ obey a summation rule. The summation rule is that the summation of the $F_{ab, cd}$ around any closed circuit of edges on the energy level cube is equal to zero. This rule can be used to compute $F_{cd, cd}$. This is important because the line irradiated in a double resonance experiment can not be observed directly. As an example, $F_{84, 84}$ may be obtained by applying the summation rule to faces 8437 or 8426 of the energy level cube. Using the 8437 face

$$F_{84, 84} = -(F_{43, 84} + F_{37, 84} + F_{78, 84}) \quad . \tag{36}$$

Using the 8426 face

$$F_{84, 84} = -(F_{42, 84} + F_{26, 84} + F_{68, 84}) \quad . \tag{37}$$

Therefore, the experimental value of $F_{84, 84}$ is obtained by taking the average of these two values. The $G_{ab, cd}$ obey the same kind of summation rule. This will affect the number of independent $G_{ab, cd}$. There are 144 $G_{ab, cd}$ for a three spin system. There are 12 lines one can irradiate, and hence 12 double resonance experiments. The summation rule shows that for each double resonance experiment, there are in general 7 independent $G_{ab,cd}$. Therefore, for a general three spin system there are 84 independent $G_{ab,cd}$.

## B. Algebraic Solution for a Weakly Coupled Three Spin System

In this section we obtain algebraic solutions for the $G_{ab,cd}$ assuming the weakly coupling limit. In this calculation, the intramolecular dipolar interaction is considered only for the AB pair. Then this interaction can be treated like an AB two spin system.[7] In vinyl bromide this amounts to neglecting the dipolar interactions involving the X proton (i.e. AX and BX pairs). As for the random field interaction, it is seen from equation (15) that $R_{abcd}$ is independent of the correlation constants in the weakly coupled limit. TA and TB are assumed equal because the A and B nuclei are attached to the same carbon atom.

Using this relaxation model and assuming the weak coupling limit, it is seen that there are relations between different double resonance experiments. This reduces the number of independent double resonance experiments to two for the X lines, one for the B lines and one for the A lines. The $G_{ab,cd}$ for irradiating X1 are related to the $G_{ab,cd}$ for irradiating X4, and the $G_{ab,cd}$ for irradiating X3 are related to the $G_{ab,cd}$ for irradiating X2. Therefore there are only two independent double resonance experiments on the X lines. When B4, B3, B2 and B1 are irradiated, all the $G_{ab,cd}$ are related, therefore there is only one independent double resonance experiment on the B lines. All the $G_{ab,cd}$ are related when A4, A3, A2 and A1 are irradiated. Therefore, there is only one independent double resonance experiment for the A lines. The symmetry relations will be explicitly shown in the following.

When X1 is irradiated, there are the following symmetry relations:

$$G_{43,84} = G_{42,84} = -G_{86,84} = -G_{87,84} \;, \tag{38}$$

$$G_{31,84} = G_{21,84} = -G_{65,84} = -G_{75,84} \;, \tag{39}$$

and

$$G_{73,84} = G_{62,84}. \tag{40}$$

These symmetry relations also hold for $F_{ab,cd}$ when X1 is irradiated by the second rf. By using the summation rule on the 3157 face and the symmetry properties, the following relation is obtained:

$$G_{31,84} + G_{15,84} + G_{57,84} + G_{73,84}$$

$$= G_{31,84} - G_{51,84} - G_{75,84} + G_{73,84}$$

$$= G_{31,84} - G_{51,84} + G_{31,84} + G_{73,84}$$

$$= G_{31,84} + G_{73,84} - G_{51,84} = 0 \;.$$

Therefore,

$$G_{31,84} = \tfrac{1}{2}(G_{51,84} - G_{73,84}) \tag{41}$$

and there are only three independent $G_{ab',ab}$ when X1 is irradiated by the second rf.

In a similar manner, there are only three independent $G_{ab,cd}$ when X4 is irradiated by the second rf. These three independent $G_{ab,cd}$ can be related to those for irradiating X1 as follows:

$$G_{65,51} = G_{43,84};\ G_{62,51} = G_{73,84};\ \text{and}\ G_{84,51} = G_{51,84} \quad . \tag{42}$$

Similarly, there are three independent $G_{ab,\,cd}$ when X3 or X2 is irradiated by the second rf. They have the following relations:

$$G_{84,73} = G_{51,62};\ \ G_{62,73} = G_{73,62};\ \text{and}\ \ G_{87,73} = G_{21,62} \quad . \tag{43}$$

The $G_{ab,\,cd}$ when irradiating B4 and B2 have the following relations:

$$\begin{aligned} &G_{42,42} = G_{86,86};\ G_{84,42} = -G_{84,86};\ G_{62,42} = -G_{62,86};\\ &G_{42,42} = G_{87,86};\ G_{21,42} = G_{65,86};\ G_{87,42} = G_{43,86}\ \ \text{and}\\ &G_{65,42} = G_{21,86}. \end{aligned} \tag{44}$$

The $G_{ab,\,cd}$ chosen here are seven independent $G_{ab,\,cd}$ as may be seen by using the summation rule. Therefore, all of the $G_{ab,\,cd}$ for irradiating B4 and B2 are related. The $G_{ab,\,cd}$ for irradiating B4 and B3 have the following relations:

$$\begin{aligned} &G_{42,42} = G_{31,31};\ G_{84,42} = -G_{51,31};\ G_{62,42} = -G_{73,31};\\ &G_{43,42} = G_{21,31};\ G_{21,42} = G_{43,31};\ G_{87,42} = G_{65,31};\ \ \text{and}\\ &G_{65,42} = G_{87,31} \ . \end{aligned} \tag{45}$$

The $G_{ab,cd}$ chosen here are seven independent $G_{ab,cd}$ as may be seen by using the summation rule. Therefore, all the $G_{ab,cd}$ for irradiating B4 and B3 are related. The relations of $G_{ab,cd}$ for irradiating B3 and B1 are similar to the relations of $G_{ab,cd}$ for irradiating B4 and B2. From the above analysis, it is seen that all the $G_{ab,cd}$ for irradiating B4, B3, B2 and B1 are related. Therefore, there is only one independent B double resonance experiment.

Because of the symmetry between the A and B protons, it can be seen that all the $G_{ab,cd}$ for irradiating A4, A3, A2 and A1 are related in the same manner as the $G_{ab,cd}$ for the B lines. Hence, there is also only one independent A double resonance experiment.

Let us choose the double resonance experiment where X1 is irradiated as an example to discuss the $G_{ab,cd}$ in detail. The population changes of each energy level have the following relations when X1 is irradiated by the second rf,

$$\chi_8 = -\chi_4 \, ; \chi_6 = \chi_7 = -\chi_2 = -\chi_3 ; \chi_5 = -\chi_1 \tag{46}$$

This reduces the number of unknowns to three. Therefore, three couples equations are obtained in matrix form:

$$\begin{vmatrix} -(2W_{1A}+2W_X+W_2) & & W_2 \\ W_{1A} & -(2W_X+2W_{1A}) & W_{1A} \\ W_2 & 2W_{1A} & -(2W_{1A}+W_2+2W_X) \end{vmatrix} \begin{vmatrix} T1 \\ T3 \\ T4 \end{vmatrix} = \begin{vmatrix} 0 \\ 0 \\ -2 \end{vmatrix} \tag{47}$$

where $$W_{1A} = W_1 + W_A \; ; \; W_A = W_B ;$$

$$W_2 = \frac{2}{5TD} \; ; \; W_1 = \frac{1}{10TD} \; ;$$

$$W_A = \frac{1}{2TA} = R_{1122} = R_{1133} = R_{4433} = R_{4422}$$

$$= R_{2211} = R_{3311} = R_{3344} = R_{2244} \; ;$$

$$W_X = \frac{1}{2TX} = R_{1155} = R_{5511} = R_{3377} = R_{7733}$$

$$= R_{4488} = R_{8844} .$$

The solutions are

$$T_1 = K(W_{1A}^2 + W_{1A}W_2 + W_X W_2) \tag{48}$$

$$T_3 = K(W_X W_{1A} + W_{1A}^2 + W_{1A}W_2) \tag{49}$$

and

$$T_4 = K(2W_X^2 + W_{1A}^2 + 4W_X W_{1A} + W_X W_2 + W_{1A}W_2 \tag{50}$$

where $K = -\frac{4}{\Delta}$ and

$$\Delta = -8W_X(W_X + W_{1A} + W_2)(W_X + 2W_{1A}) .$$

To simplfy the following discussion, let us assume that $W_A = W_B = W_X$. Then $G_{ab,cd}$ can be expressed in terms of a single parameter, r, where

$$r = \frac{W_X}{W_1} = \frac{5TD}{TX} \tag{51}$$

From equation (48), (49), (50), (51) and $W_2 = 4W_1$, the $G_{ab,cd}$ are obtained as follows:

$$G_{73,74} = \frac{-(2r^2+7r+5)}{7r^2+14r+5} \quad , \tag{52}$$

$$G_{51,84} = \frac{-(r^2+10r+5)}{7r^2+14r+5} \quad , \tag{53}$$

and

$$G_{43,84} = \frac{5r^2+7r}{2(7r^2+14r+5)} \quad , \tag{54}$$

$$G_{31,84} = \frac{r^2-3r}{2(7r^2+14r+5)} \quad . \tag{55}$$

In order to estimate the contribution of intramolecular and intermolecular-dipolar interactions, $G_{ab,cd}$ can be plotted as function of the fractional contribution of intramolecular dipolar interaction. The fractional contribution of intramolecular interaction, F, is defined as

$$F = \frac{\frac{1}{TD}}{\frac{1}{TD} + \frac{1}{TX}} = \frac{5}{5+r} \quad . \tag{56}$$

Figure 2 shows $G_{43,84}$, $G_{73,84}$, $G_{51,84}$ and $G_{31,84}$ as a function of F. $G_{73,84}$ monotonically decreases from -.29 at F = 0 to -1.0 at F = 1. This may be qualitatively explained as follows using the energy cube in Figure 1. When $\chi 1$

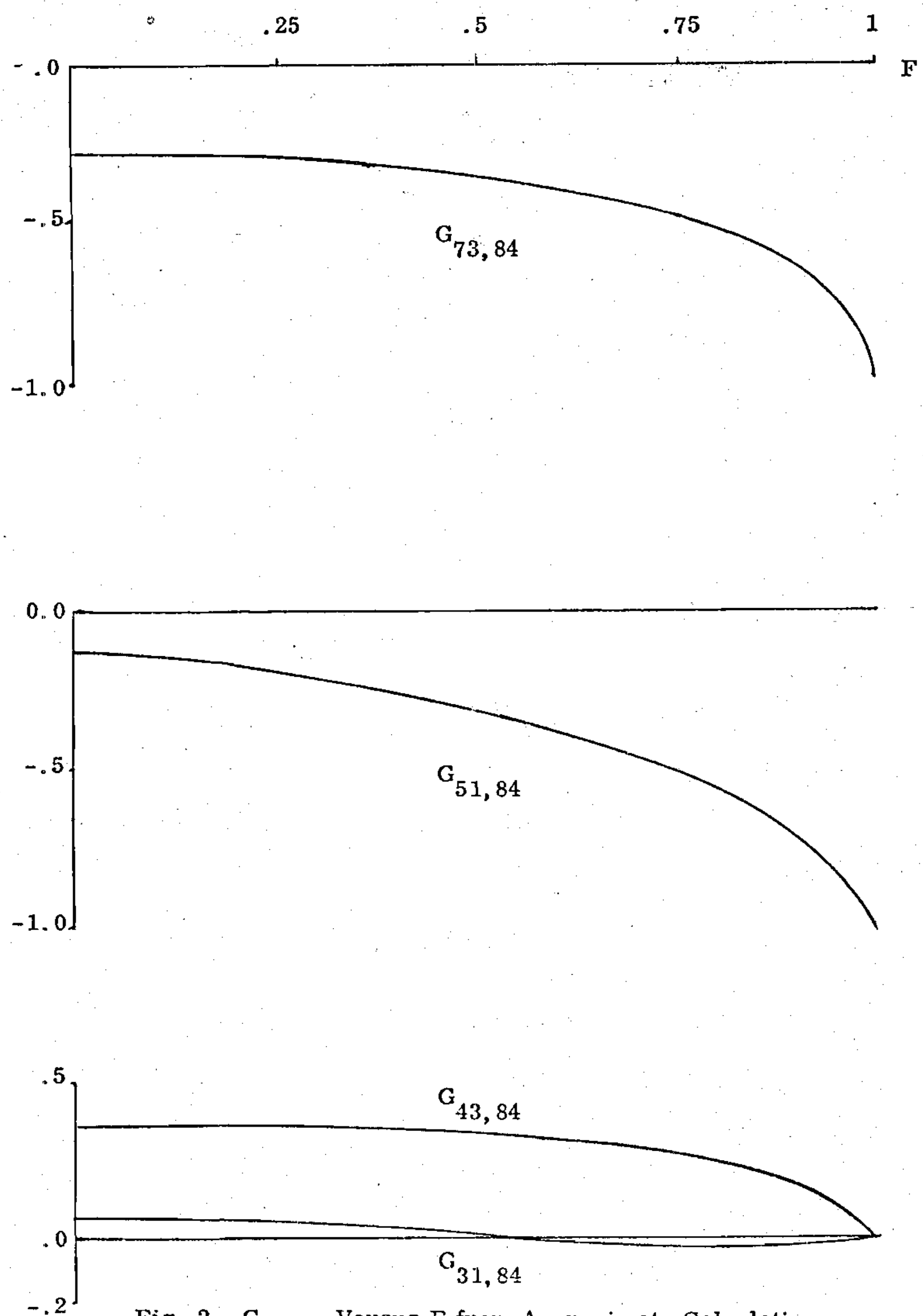


Fig. 2. $G_{ab,84}$ Versus F from Approximate Calculation.

is irradiated, $\chi_4$ is + and $\chi_8$ is −. When F = 0, $\chi_7$ will be more negative than $\chi_3$ because $\chi_7$ is connected to $\chi_8$ by A3 and $\chi_3$ is connected to $\chi_4$ by A4. Hence, $G_{73,84}$ is negative when F = 0. When F = 1, $\chi_7$ will be much more negative than $\chi_3$ because $\chi_7$ is connected to $\chi_8$ and in addition to $\chi_5$ which is connected to $\chi_8$ by the strong 5→8 double quantum transition, and $\chi_3$ is connected to $\chi_4$ and in addition to $\chi_1$, which is connected to $\chi_4$ by the strong 1→4 double quantum transition. Hence, $G_{73,84}$ is much more negative at F = 1.

$G_{51,84}$ decreases from −.14 at F = 0 to −1.0 at F = 1. When X1 is irradiated, $\chi_4$ is + and $\chi_8$ is −. When F = 0, $\chi_5$ is more negative than $\chi_1$ because $\chi_5$ is indirectly connected to $\chi_8$ by B1 and A3 and $\chi_1$ is indirectly connected to $\chi_4$ by B3 and A4. Hence, $G_{51,84}$ is negative when F = 0. When F = 1, $\chi_5$ will be much more negative than $\chi_1$ because $\chi_5$ is directly connected to $\chi_8$ by strong double quantum transition 5→8 and $\chi_1$ is directly connected to $\chi_4$ by strong double quantum transition 1→4. Hence, $G_{51,84}$ is much more negative at F = 1.

$G_{43,84}$ monotonically decreases from .36 at F = 0 to 0 at F = 1. When X1 is irradiated $\chi_4$ is + and $\chi_8$ is −. When F = 0, $\chi_4$ will be more positive than $\chi_3$ because $\chi_3$ is indirectly connected to $\chi_8$ by $X_3$ and A3. Hence, $G_{43,84}$ is positive when F = 0. When F = 1, $\chi_4$ is connected to $\chi_1$ by the strong double quantum transition 4→1 and $\chi_3$ is connected $\chi_1$ by B3. Hence, $G_{43,84}$ becomes 0 at F = 1.

$G_{31,84}$ monotonically decreases from .071 at F = 0 to 0 at F = .53. $G_{31,84}$ becomes negative when F continues to increase and finally goes back to zero at F = 1. When X1 is irradiated $\chi_4$ is + and $\chi_8$ is −. When F = 0, $\chi_3$ will be more positive than $\chi_1$ because $\chi_3$ is connected to $\chi_4$. Hence, $G_{31,84}$ is positive when

$F = 0$. When $F > .53$, $\chi_1$ will be more positive than $\chi_3$ because $\chi_1$ is connected to $\chi_4$ by the strong double quantum transition $4 \rightarrow 1$. Hence, $G_{31,84}$ is negative when $F > .53$. When $F = 1$, $\chi_3$ is equal to $\chi_1$ because $\chi_3$ is connected to $\chi_4$ and $\chi_1$, and $\chi_1$ and $\chi_4$ are connected by strong double quantum transitions $4 \rightarrow 1$. Hence, $G_{31,84}$ is 0 at $F = 1$. The magnitude of $G_{31,84}$ is always close to zero and therefore is not useful.

### C. Computer Solution

Equation (30), (31) and (32) can be expressed in matrix form as

$$RT = K \tag{57}$$

where R is a symmetric matrix. Equation (57) can be solved by using the transformation U which diagonalizes R, i.e.

$$\bar{R} = U^{-1}RU, \; \bar{R}_{ab} = r_a \delta_{ab} \tag{58}$$

Then, the transform of equation (57) is

$$\bar{R}\bar{T} = \bar{K} \tag{59}$$

where

$$\bar{T} = U^{-1}T \text{ and} \tag{60}$$

$$\bar{K} = U^{-1}K \tag{61}$$

The transform $\bar{T}$ is given by

$$\bar{T}_a = \frac{\bar{K}_a}{r_a} \tag{62}$$

and

$$T = U\bar{T} \tag{63}$$

The difficulty with the above is that $r_1 = 0$. However, $\bar{K}_1 = 0$ also. This is because

$$\bar{K}_1 = \sum_j (U^{-1})_{1j} K_j = \sum_j U_{j1} K_j$$
$$= \frac{1}{\sqrt{N}} \sum_{j=1}^{N} K_j = 0$$

Therefore, the general solution of (57) can be written as

$$G_a = \sum_{l \neq 1} r_l^{-1} U_{al} \sum_{m=1}^{N} U_{ml} K_m \tag{64}$$

The sum over l in (64) does not include $l = 1$ and is restricted to values of l for which $r_l \neq 0$. It is useful to note that these terms could be included with arbitrary values for the corresponding $a_l^{-1}$. In this case, the off diagonal elements of $\chi$ would not be affected, and a constant would be added to each diagonal element of $\chi$. This would not affect the computed values because only the differences between diagonal elements appear in subsequent computations. This is explicitly seen in the calculation of $G_{ab,cd}$ and $F_{ab,cd}$ in equations (35) and (34), respectively. The advantage of this calculation is that only one U is needed for all 12 double resonance experiments. This method agreed with the full calculation using the formalism of Part One to three significant figures. This calculation for a tightly coupled three spin system will be discussed in Chapter IV.

# CHAPTER IV

# EXAMPLE: VINYL BROMIDE

## A. Experimental

### 1. Samples

Vinyl bromide is used to illustrate the Overhauser effects of an ABX three spin system. Two samples were prepared for this experiment. The first sample was prepared with 10% v vinyl bromide in $CS_2$ solution. For a locking signal, 5% v TMS was added to this sample. This sample was degassed by the usual freeze-thaw method. We shall call this sample A in the following.

The second sample was prepared in a standard 5-mm-o.d. NMR tube fitted with a standard taper joint and ground glass stopper. This sample was prepared with 10% v vinyl bromide in $CS_2$ solution. For a locking signal, 5% v TMS was added to this sample. Oxygen gas was bubbled into this sample. We shall call this sample B in the following. The relaxation of sample B will be dominated by the intermolecular dipolar interaction of oxygen.

### 2. Instrumentation

The instrumentation for this experiment was the same as in reference 1 except that the input to the phase detector was connected to the $H_2$ modulation output through a Hewlett Packard 250-D attenuator and a PAR Model JB-5 lock-in amplifier. This feed-back signal was used to cancel the response due to $H_2$. The lock-in amplifier was used to control the phase of the feed-back signal. The phase and amplitude of the feedback signal were adjusted to completely cancel the response to $H_2$. The experiment did not show complete cancellation. This might have been due to the instability of the frequency and phase.

## B. Spectra and Spectral Parameters for Samples A and B

The chemical shifts and coupling constants of vinyl bromide were obtained by fitting the observed frequency and intensity of each line with computed values. Table 1 shows the calculated and observed frequencies and intensities of all lines. A single resonance spectrum is shown in Figure 3. The A and B protons are attached to the first carbon atom. The X proton and bromine atom are attached to the second atom. The larmor frequency of the X proton is used as the reference for the measurement of all frequencies. The intensity of each line measured is relative to X4 line. The chemical shifts and coupling constants of vinyl bromide were found as:

$$\delta_{AB} = 15 \pm .1\ H_z\ ;\ \delta_{AX} = 63.7 \pm .1\ H_z\ ;$$

$$\delta_{BX} = 48.7 \pm .1\ H_z;\ J_{AB} = -1.7 \pm .1\ H_z\ ;$$

$$J_{AX} = 15.2 \pm .1\ H_z;\ J_{BX} = 7.2 \pm .1\ H_z.$$

These results are in good agreement with previously reported values.[21] Table 2 shows the expansion coefficients of the eigenkets $|a>$, $|b>\ldots$ with respect to the product kets $|M_X M_B M_A>$, and the energy for each eigenket. In the weakly coupled limit $|a>$, $|b>\ldots$ correspond to $|1>$, $|2>\ldots$ respectively. In the first column, $\pm\frac{1}{2}$ is denoted by $\pm$. The energy for each ket is given in the bottom row.

Table 1. The Calculated and Observed Frequencies and Intensities of Vinyl Bromide

| | Frequencies ($H_Z$) | | Intensities | |
|---|---|---|---|---|
| | Calculated | Observed | Calculated | Observed |
| X4 | -12.269 | -12.1 | 1.000 | 1.00 |
| X3 | - 5.258 | - 5.2 | 1.280 | 1.29 |
| X2 | 2.940 | 2.9 | 1.545 | 1.56 |
| X1 | 9.951 | 9.9 | 2.130 | 2.09 |
| B4 | 44.644 | 44.5 | 1.626 | 1.75 |
| B3 | 46.164 | 46.1 | 1.788 | 1.96 |
| B2 | 51.655 | 51.5 | 1.064 | 1.24 |
| B1 | 53.175 | 53.2 | 1.487 | 1.67 |
| A4 | 56.285 | 56.3 | 1.993 | 2.40 |
| A2 | 57.805 | 57.7 | 1.681 | 2.01 |
| A3 | 71.494 | 71.5 | 1.277 | 1.57 |
| A1 | 73.014 | 73.0 | 1.003 | 1.25 |

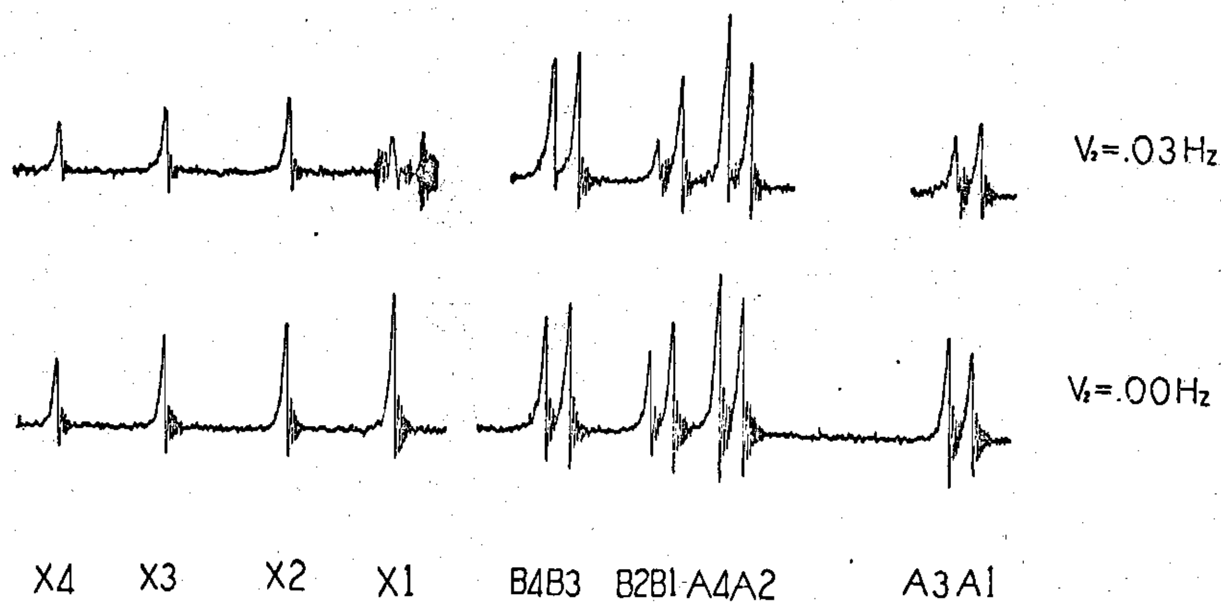


Fig. 3. Single and Double Resonance Traces of Sample A with $H_2(t)$ at X1.

Table 2. The Expansion Coefficients of the Eigenkets $|a>, |b> \ldots,$ with Respect to Product Kets $|M_X M_B M_A>$, and the Energy for Each Eigenket

| MX | MB | MA | a | b | c | d | e | f | g | h |
|---|---|---|---|---|---|---|---|---|---|---|
| − | − | − | 1.00 | 0 | 0 | 0 | 0 | 0 | 0 | 0 |
| − | − | + | 0 | .993 | .032 | 0 | .110 | 0 | 0 | 0 |
| − | + | − | 0 | −.039 | .997 | 0 | −.063 | 0 | 0 | 0 |
| − | + | + | 0 | 0 | 0 | .989 | 0 | −.074 | −.129 | 0 |
| + | − | − | 0 | .107 | .067 | 0 | .992 | 0 | 0 | 0 |
| + | − | + | 0 | 0 | 0 | .083 | 0 | .994 | .065 | 0 |
| + | + | − | 0 | 0 | 0 | .123 | 0 | −.075 | .990 | 0 |
| + | + | + | 0 | 0 | 0 | 0 | 0 | .0 | 0 | 1 |
| $E_o$ | | | $3/2\nu_{oX}$ | $\frac{1}{2}\nu_{oX}$ | $\frac{1}{2}\nu_{oX}$ | $\frac{1}{2}\nu_{oX}$ | $\frac{1}{2}\nu_{oX}$ | $-\frac{1}{2}\nu_{oX}$ | $-\frac{1}{2}\nu_{oX}$ | $-3/2\nu_{oX}$ |
| $(H_Z)$ | | | −116.60 | −15.13 | −26.77 | +73.33 | −85.20 | 31.63 | 11.79 | 126.95 |

Fig. 3 shows single and double resonance spectra of sample A. A single resonance spectrum is on the bottom trace. Each line is well separated. A double resonance spectrum is on the top trace. In this double resonance experiment, the X1 line is irradiated. The strength of $H_2$ is .03 $H_z$. This was obtained analyzing strong irradiation double resonance spectra of 1, 1, 2-trichloroethane for one fixed strength of modulation. This calibrated $H_2$ was attenuated to .03 $H_z$ with a Hewlett Packard 250-D attenuator. The beat pattern is caused by the response of $H_2$.

Fig. 4 shows single and double resonance spectra of sample B. A single resonance spectrum is on the bottom trace. Although each line is broader than the corresponding line in sample A, they are still well separated. The broadening is caused by the dissolved oxygen gas in this sample. The oxygen causes a strong intermolecular dipolar interaction. A double resonance spectrum is shown on the top trace. The X1 line is irradiated with a strength of .076 $H_z$.

## C. Dependence of $G_{ab,cd}$ on F for Vinyl Bromide

For intramolecular dipolar interaction, the structural parameters are listed below:

$$r_{ab} = 1.73\ \mathring{A};\ r_{bx} = 2.34\ \mathring{A};\ r_{ax} = 2.98\ \mathring{A};$$

$$\angle HCH = 120^{\circ} \text{ and } \angle HCC = 120^{\circ}.$$

The $g_{NN'}$ of equation (11) are calculated from the structural parameters as follows. The AB, BX and AX pairs are numbered as 1, 2 and 3, respectively.

$$g_{11} = .2000;\ g_{22} = .0327;\ g_{33} = .0077;$$

$$g_{12} = -.0405;\ g_{13} = -.0050 \text{ and } g_{23} = .0100.$$

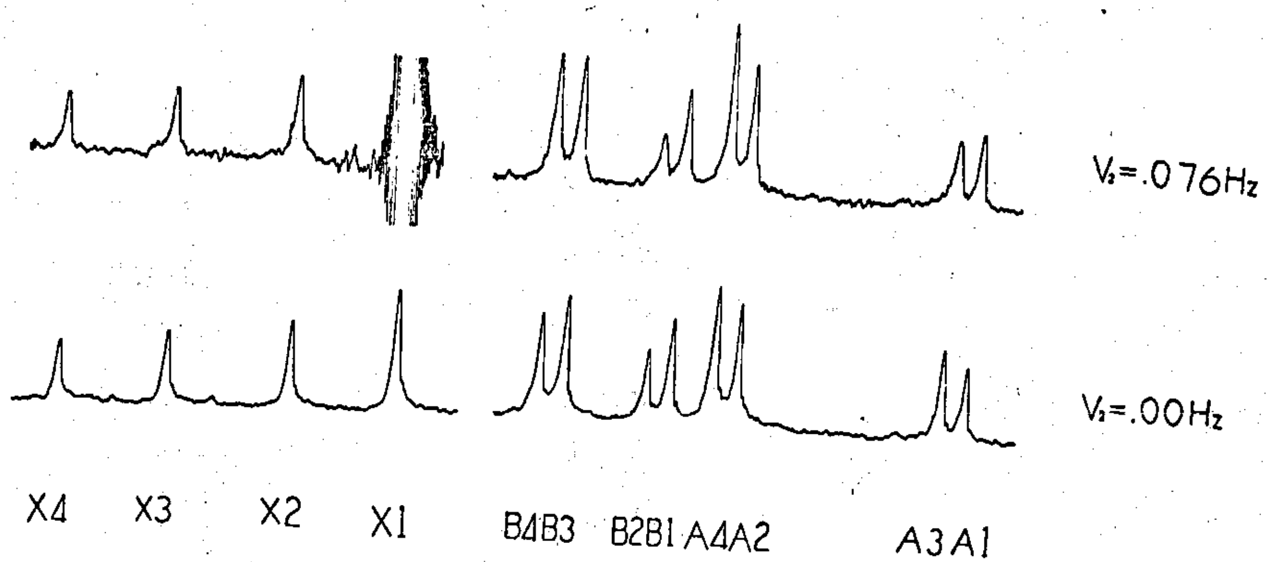


Fig. 4. Single and Double Resonance Traces of Sample B with $H_2(t)$ at X1.

For the intermolecular dipolar interactions; TA, TB and TX are assumed equal because of the small distances between them and the rigid structure of vinyl bromide. The correlation constants are assumed to be $C_{AB} = 1$, $C_{BX} = 0$ and $C_{AX} = 0$. The experimental and theoretical results are not sensitive to the variation of correlation constants.

The $G_{ab, cd}$ are plotted as a function of F by assuming $C_{AB} = 1$, $C_{BX} = 0$, $C_{AX} = 0$ and TA = TB = TX. The curves were computed assuming TD = 18 sec., however, the computed results depend only on TD/TX. Figure 5 indicates the plots of $G_{73, 84}$, $G_{51, 84}$, $G_{43, 84}$ and $G_{31, 84}$ versus F from the exact calculation. Figure 6 shows seven independent $G_{ab, 86}$ versus F from an exact calculation. The independent $G_{ab, 86}$ chosen here have the best sensitivity to the experimental results. Figure 7 shows seven independent $G_{ab, 87}$ versus F from exact calculation. The independent $G_{ab, 87}$ chosen here have the best sensitivity to the experimental results.

The curves in Figure 5 can be compared with the corresponding curves in Figure 2. For the extreme case at F = 1, these curves are quite different. For example, $G_{73, 84}$ in Fig. 5 is -.44 and $G_{73, 84}$ in Fig. 2 is -1.0 at F = 1.0. The difference results because now $\chi_3$ is connected to $\chi_8$ by the $3 \rightarrow 8$ double quantum transition of the AX pair. This makes $\chi_3$ less positive, hence, $G_{73, 84}$ less negative.

$G_{51, 84}$ in Fig. 5 is -.65 and $G_{51, 84}$ in Fig. 2 is -1 at F = 1. The difference results because $\chi_1$ is connected to $\chi_6$ by the $1 \rightarrow 6$ double quantum transition of the AX pair. $\chi_1$ is less positive, hence $G_{51, 84}$ is less negative.

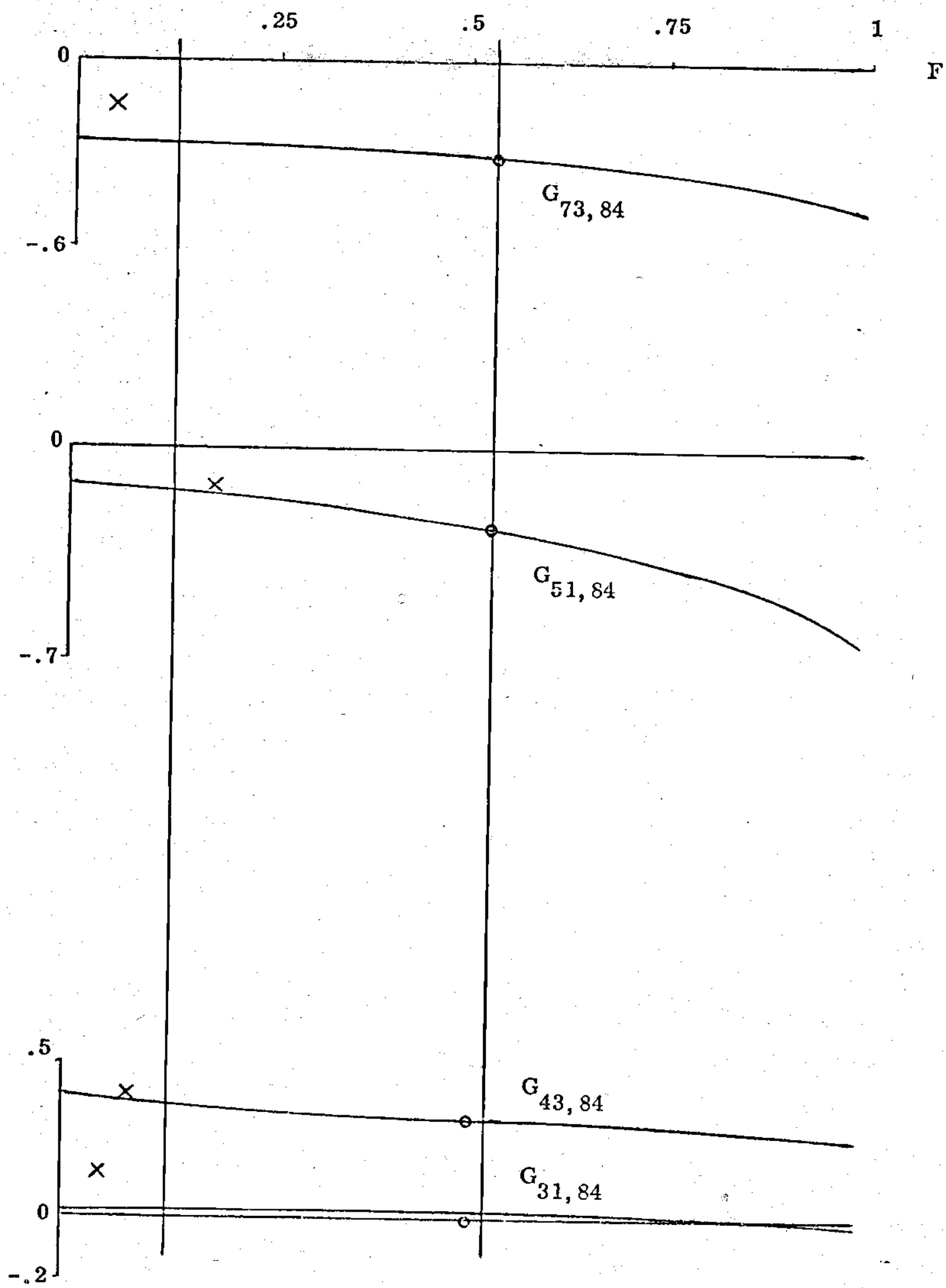


Fig. 5. $G_{ab,84}$ Versus F from Exact Calculation.

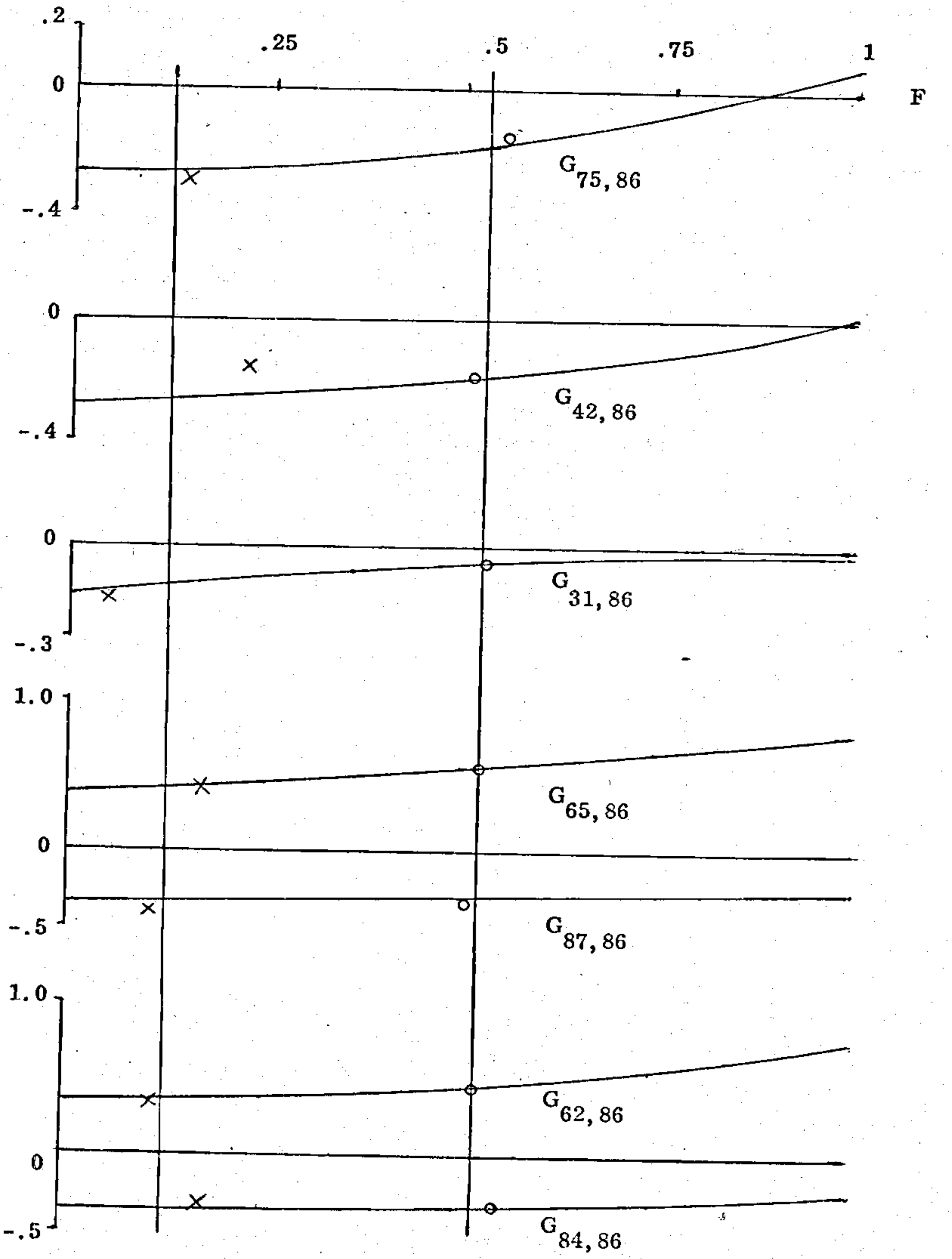


Fig. 6. $G_{ab,86}$ Versus F from Exact Calculation.

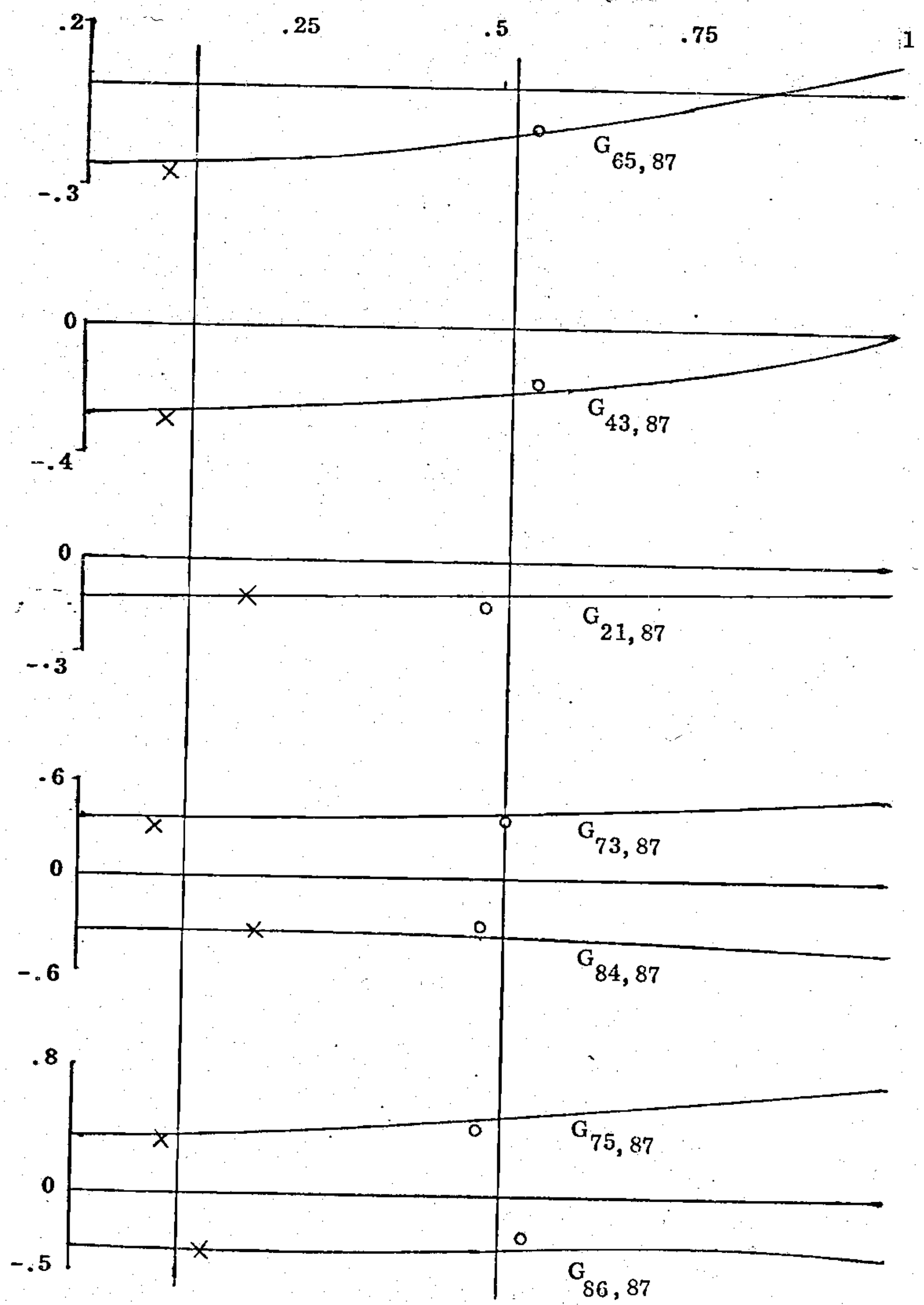


Fig. 7. $G_{ab,87}$ Versus F from Exact Calculation.

$G_{43,84}$ in Fig. 5 is .25 and the $G_{43,84}$ in Fig. 2 is 0 at F = 1. The difference results because $\chi_3$ is connected to $\chi_8$ by the $3 \rightarrow 8$ double quantum transition of the AX pair. $\chi_3$ is less positive, hence $G_{43,84}$ in Fig. 5 is more positive than in Fig. 2.

The magnitude of the $G_{31,84}$ in Fig. 5 is less than the $G_{31,84}$ in Fig. 2. This results because $\chi_3$ is connected to $\chi_8$ by the $3 \rightarrow 8$ double quantum transition and $\chi_1$ is connected to $\chi_6$ by the $1 \rightarrow 6$ double quantum transition. Both $\chi_3$ and $\chi_1$ are less positive, hence the magnitude of $G_{31,84}$ in Fig. 5 is less than in Fig. 2.

From this analysis, it is seen that there is a substantial effect when the intramolecular dipolar mechanism is important. The plots in Figs. 6 and 7 can all be explained qualitatively in a manner similar to the discussion given for Fig. 2 in section IIIB. In Figs. 6 and 7, $G_{75,86}$, $G_{65,86}$, $G_{62,86}$, $G_{65,87}$, $G_{43,87}$ and $G_{75,87}$, are the most sensitive curves.

The curves in Figs. 5, 6 and 7 will be used to determine contributions to relaxation from intramolecular and intermolecular dipolar interactions for the samples A and B.

## D. Results

The experimental results for the samples were expressed as relative fractional change of intensities and compared with the calculated curves in Figs. 5, 6 and 7. By obtaining the best fit with the calculated curves, F was obtained for each sample. The $F_{ab,cd}$ were used to obtain TD and TX. This gave an independent check on the value of F obtained from the $G_{ab,cd}$.

1. Sample A

Double resonance experiments were carried out on all twelve lines of sample A. The line heights for single and double resonance are given in Table 3. In addition, the double resonance line widths, $W^D$, are given when deviations from the single resonance line widths occur. The line width of each single resonance transition was .37 $H_z$. The lines irradiated by the second rf with strength .03 $H_z$ are given at the left hand side of the table. The lines observed are given at the top of the table. The observed single resonance signal heights, $I^{SR}$, are given at the bottom of the table. Each entry has two values. The value on the top is the signal height of the double resonance line, $I^{DR}$. The value on the bottom is the width of double resonance line, $W^{DR}$. There are no entries for the irradiated lines and some lines near the irradiated lines because they are covered by beat patterns. The $G_{ab,cd}$ for the twelve double resonance experiments are listed in Table 4. The lines irradiated by the second rf with strength .03 $H_z$ are given at the left hand side of the table. The lines observed are given at the top of the table. Each entry has two values: the calculated value is on the top, the experimental value is on the bottom. Since the calculation does not consider the effects of intensity from the splitting and field inhomogeneity, the observed double resonance line heights were corrected as follows:

$$I^{DR} = I^{DR} \times \frac{W^D}{W^S} , \qquad (65)$$

where $I^{DR}$ and $W^D$ are the signal height and width respectively in the double resonance trace, and $W^S$ is the width in the single resonance trace. The lines subjected

Table 3. $I^{SR}$, $I^{DR}$ and $W^D$ of Sample A

| | | X4 (51) | X3 (73) | X2 (62) | X1 (84) | B4 (42) | B3 (31) | B2 (86) | B1 (75) | A4 (43) | A2 (21) | A3 (87) | A1 (65) |
|---|---|---|---|---|---|---|---|---|---|---|---|---|---|
| X4 | $I^{DR}$ | | 3.20 | 4.35 | 6.05 | 5.6 | 4.48 | 4.43 | 7.13 | 7.43 | 4.35 | 5.25 | 5.28 |
| (51) | $W^D$ | | .39 | | | .36 | .43 | | | | | | |
| X3 | $I^{DR}$ | 2.60 | | 4.65 | 5.38 | 6.00 | 8.30 | 3.95 | 3.53 | 4.85 | 6.05 | 6.23 | 4.33 |
| (73) | $W^D$ | .36 | | | .38 | | .36 | | .44 | .44 | | .37 | |
| X2 | $I^{DR}$ | 2.60 | 3.77 | | 5.50 | 3.40 | 6.00 | 5.23 | 5.73 | 7.58 | 7.58 | 4.70 | 2.18 |
| (62) | $W^D$ | .36 | | | | .46 | | .38 | | .39 | .40 | .38 | .49 |
| X1 | $I^{DR}$ | 2.74 | 3.38 | 4.06 | | 6.48 | 6.63 | 2.33 | 5.38 | 8.75 | 6.80 | 2.93 | 3.85 |
| (84) | $W^D$ | | | | | | | | | | | | |
| B4 | $I^{DR}$ | 3.40 | 4.80 | 3.23 | 8.48 | | 5.43 | 3.13 | 5.08 | 4.83 | 8.13 | 4.93 | 4.65 |
| (42) | $W^D$ | | | .41 | .38 | | | .41 | .38 | .46 | .40 | | |
| B3 | $I^{DR}$ | 2.00 | 5.70 | 5.03 | 7.90 | 4.73 | | 3.83 | 4.83 | 9.53 | 4.00 | 5.53 | 4.75 |
| (31) | $W^D$ | .44 | | | | | | | | .40 | .46 | | .3 |
| B2 | $I^{DR}$ | 3.45 | 3.95 | 6.38 | 4.68 | 4.88 | 6.05 | | 5.18 | 7.75 | 7.1 | 3.68 | 5.23 |
| (86) | $W^D$ | | .38 | .37 | .43 | .38 | .38 | | | .36 | | .41 | .38 |
| B1 | $I^{DR}$ | 4.25 | 3.05 | 5.83 | 7.1 | 5.53 | 5.73 | 3.60 | | 8.10 | 6.70 | 6.80 | 2.53 |
| (75) | $W^D$ | | .38 | .34 | | | | | | .38 | | .36 | .46 |
| A4 | $I^{DR}$ | 3.23 | 2.88 | 5.23 | 7.43 | 4.10 | 7.43 | 3.95 | 5.73 | | 6.50 | 4.20 | 3.78 |
| (43) | $W^D$ | | | .36 | .41 | .39 | .44 | .36 | .38 | | | .39 | .38 |
| A2 | $I^{DR}$ | 1.85 | 4.08 | 6.10 | 6.85 | 7.43 | 3.63 | 4.48 | 5.58 | 5.85 | | 4.78 | 3.53 |
| (21) | $W^D$ | .48 | | .39 | .39 | .38 | | | | | | .36 | .36 |
| A3 | $I^{DR}$ | 3.30 | 5.10 | 4.88 | 5.20 | 5.70 | 6.50 | 3.03 | 6.05 | 6.73 | 6.20 | | 3.90 |
| (87) | $W^D$ | | .38 | | .36 | | .38 | .39 | .38 | | | | |
| A1 | $I^{DR}$ | 4.10 | 4.48 | 2.95 | 6.63 | 6.53 | 6.55 | 5.45 | 3.68 | 7.60 | 6.00 | 4.45 | |
| (65) | $W^D$ | | | .46 | .36 | | | | .44 | | | | |
| | $I^{SR}$ | 3.40 | 4.38 | 5.30 | 7.10 | 5.95 | 6.68 | 4.20 | 5.68 | 8.15 | 6.83 | 5.35 | 4.25 |

Table 4. $G_{ab, cd}$ of Sample A

| | X4 (51) | X3 (73) | X2 (62) | X1 (84) | B4 (42) | B3 (31) | B2 (86) | B1 (75) | A4 (43) | A2 (21) | A3 (87) | A1 (65) |
|---|---|---|---|---|---|---|---|---|---|---|---|---|
| X4 | -1 | -.3129 | -.3170 | -.2820 | -.0095 | -.3279 | .0255 | .3592 | -.0317 | -.3502 | -.0008 | .3328 |
| (51 | -1 | -.30 | -.28 | -.23 | -.05 | -.30 | .08 | .41 | -.14 | -.34 | -.03 | .38 |
| X3 | -.2814 | -1 | -.1654 | -.2863 | .0688 | .3913 | -.0522 | -.3271 | -.3813 | -.0587 | .3322 | .0574 |
| (73) | -.29 | -1 | -.13 | -.28 | .01 | .42 | -.09 | -.32 | -.38 | -.16 | .32 | .01 |
| X2 | -.2786 | -.1612 | -1 | -.2785 | -.3347 | -.0486 | .3869 | .0688 | .0688 | .3419 | -.0615 | -.3796 |
| (62) | -.28 | -.18 | -1 | -.30 | -.32 | -.13 | .38 | .01 | .05 | .36 | .08 | -.37 |
| X1 | -.2805 | -.3155 | -.3147 | -1 | .3508 | .0323 | -.3345 | -.0025 | .3300 | .0114 | -.3546 | -.0226 |
| (84) | -.26 | -.31 | -.31 | -1 | .35 | .00 | -.35 | -.07 | .34 | .00 | -.35 | -.12 |
| B4 | -.0120 | .0824 | -.4180 | .3840 | -1 | -.1615 | -.1981 | -.0672 | -.3178 | .5208 | -.0161 | .1147 |
| (42) | 0.00 | .14 | -.41 | .39 | -1 | -.20 | -.17 | -.06 | -.30 | .51 | -.12 | .13 |
| B3 | -.3576 | .4613 | -.0622 | .0331 | -.1594 | -1 | -.0643 | -.1812 | .5210 | -.3197 | .0927 | -.0241 |
| (31) | .34 | .40 | -.07 | .15 | -.26 | -1 | -.12 | -.20 | .46 | -.29 | .04 | -.05 |
| B2 | .0266 | -.0604 | .4598 | -.3489 | -.1915 | -.0632 | -1 | -.1502 | -.0244 | .1039 | -.3129 | .5370 |
| (86) | .03 | -.07 | .45 | -.34 | -.19 | -.05 | -1 | -.16 | -.02 | .07 | -.33 | .55 |
| B1 | .4049 | -.4019 | .0876 | -.0022 | -.0702 | -.1932 | -.1600 | -1 | .1099 | -.0132 | .5097 | .3305 |
| (75) | .38 | -.38 | .09 | .00 | -.12 | -.21 | -.21 | -1 | .11 | .03 | .50 | .32 |
| A4 | -.0310 | -.4480 | .0683 | .3551 | -.3105 | .5189 | -.0237 | .1020 | -1 | -.1705 | -.1970 | -.0713 |
| (43) | -.07 | -.47 | .03 | .37 | -.32 | .52 | -.03 | .11 | -1 | -.15 | -.18 | -.07 |
| A2 | -.3758 | -.0698 | .4163 | .0123 | .5106 | -.3184 | .1066 | -.0123 | -.1710 | -1 | -.0891 | -.2080 |
| (21) | -.37 | -.10 | .39 | .01 | .49 | -.31 | .10 | -.03 | -.23 | -1 | -.11 | -.20 |
| A3 | -.0011 | .4033 | -.0769 | -.3933 | -.0156 | .0959 | -.3321 | .5003 | -.2032 | -.0918 | -1 | -.1676 |
| (87) | -.05 | .39 | -.12 | -.36 | -.06 | .06 | -.30 | .46 | -.18 | -.14 | -1 | -.14 |
| A1 | .3478 | .0688 | -.4499 | -.0251 | .1113 | -.0260 | .5358 | -.3050 | -.0652 | -.2025 | -.1592 | -1 |
| (65) | .35 | .03 | -.43 | -.05 | .17 | -.03 | .50 | -.32 | -.12 | -.20 | 0.20 | -1 |

to this correction are those lines in which the line width in the double resonance trace shows a deviation from that of the single resonance trace. The experimental $G_{ab, cd}$ listed in Table 4 were then computed using the corrected $I^{DR}$. The experiment points of $G_{ab, cd}$ are drawn in the Figs. 5, 6 and 7 as circle o. The $G_{ab, cd}$ have an experimental error of 12%. The F corresponding to the experimental point of $G_{ab, cd}$ varies between .5 to .56. One best vertical line can be drawn through the experimental points of $G_{ab, cd}$ at F = .53.

It was mentioned in section IVC that we assumed TA = TB = TX, $C_{AB} = 1$, $C_{AX} = 0$ and $C_{BX} = 0$. Therefore, the absolute TX and TD can be obtained by the best fit of experimental and calculated $F_{ab, cd}$ obtained by varying TD and TX. In computing $F_{ab, cd}$, TD was varied from 15 to 21 seconds, and TX was varied from 17 to 23 seconds. The computation assumed $C_{AB} = 1$, $C_{AX} = C_{BX} = 0$ and $H_2 = .03\ H_z$. The TD and TX for the best fit of the experimental and calculated $F_{ab, cd}$ are 18 seconds and 20 seconds, respectively. These $F_{ab, cd}$ for all twelve double resonance experiments are listed in Table 5. The lines observed are given at the top of the table. The lines irradiated are given at the left hand side of the table. Each entry has calculated and observed $F_{ab, cd}$. The calculated value is on the top of each entry and the observed value is on the bottom of each entry. The experimental $F_{ab, cd}$ were corrected for line width changes as given by equation (65).

The experimental values of $F_{ab, ab}$ are obtained from the average of equations (36) and (37). The calculated and experimental $F_{ab, ab}$ in Table 5 agree within experimental error, 8%. The experimental and calculated $F_{ab, cd}$ in Table 5 agree within experimental error, 8%. Since the absolute TD and TX can be obtained from

Table 5. $F_{ab, cd}$ of Sample A

| | X4 (51) | X3 (73) | X2 (62) | X1 (84) | B4 (42) | B3 (31) | B2 (86) | B1 (75) | A4 (43) | A2 (21) | A3 (87) | A1 (65) |
|---|---|---|---|---|---|---|---|---|---|---|---|---|
| X4 | -.5922 | -.1853 | -.1877 | -.1670 | -.0056 | -.1942 | .0151 | .2127 | -.0188 | -.2074 | -.0005 | .1971 |
| (51) | -.64 | -.19 | -.18 | -.15 | -.03 | -.19 | .05 | .26 | -.09 | -.22 | .02 | .24 |
| X3 | -.1962 | -.6971 | -.1153 | -.1996 | .0480 | .2728 | -.0364 | -.2280 | -.2658 | -.0409 | .2316 | .0400 |
| (75) | -.20 | -.69 | -.09 | -.19 | .01 | .29 | -.06 | -.22 | -.26 | -.11 | .22 | .01 |
| X2 | -.2092 | -.1210 | -.7508 | -.2091 | -.2513 | -.0365 | .2905 | .0517 | .0419 | .2567 | -.0462 | -.2850 |
| (62) | -.21 | -.14 | -.76 | -.23 | -.24 | -.10 | .29 | .01 | .04 | .27 | -.06 | -.28 |
| X1 | -.2119 | -.2383 | -.2377 | -.7554 | .2650 | .0244 | -.2527 | -.0019 | .2493 | .0086 | -.2679 | -.0171 |
| (84) | -.19 | -.23 | -.23 | -.74 | .26 | .00 | -.26 | -.05 | .25 | .00 | -.26 | -.09 |
| B4 | -.0081 | .0558 | -.2832 | .2601 | -.6774 | -.1094 | -.1342 | -.0455 | -.2153 | .3528 | -.0109 | .0777 |
| (42) | 0.00 | .10 | -.28 | .27 | -.69 | .14 | -.12 | -.04 | -.21 | .35 | -.08 | .09 |
| B3 | -.2526 | .3258 | -.0439 | .0234 | -.1126 | -.7063 | -.0454 | -.1280 | .3680 | -.2258 | .0655 | -.0170 |
| (31) | -.26 | .30 | -.05 | .11 | -.20 | -.76 | -.09 | -.15 | .35 | -.22 | .03 | -.04 |
| B2 | .0159 | -.0361 | .2749 | -.2086 | -.1145 | -.0378 | -.5979 | -.0898 | -.0146 | .0621 | -.1871 | .3211 |
| (86) | .02 | -.04 | .26 | -.20 | -.11 | -.03 | -.58 | -.09 | -.01 | .04 | -.19 | .32 |
| B1 | .2601 | -.2582 | .0563 | -.0014 | -.0451 | -.1241 | -.1028 | -.6424 | .0706 | -.0085 | .3274 | -.2123 |
| (75) | .25 | -.25 | .06 | 0.00 | -.08 | -.14 | -.14 | -.66 | .07 | -.02 | .33 | -.21 |
| A4 | -.0225 | -.3255 | .0496 | .2580 | -.2256 | .3770 | -.0172 | .0741 | -.7265 | -.1239 | -.1431 | -.0518 |
| (43) | -.05 | -.34 | .02 | .27 | -.23 | .38 | -.02 | .08 | -.73 | -.11 | -.13 | -.05 |
| A2 | -.2602 | -.0483 | .2882 | .0085 | .3535 | -.2204 | .0738 | -.0085 | -.1184 | -.6923 | -.0617 | -.1440 |
| (21) | -.26 | -.07 | .27 | .007 | .34 | -.22 | .07 | -.02 | -.16 | -.70 | -.08 | -.14 |
| A3 | -.0007 | .2503 | -.0477 | -.2441 | -.0097 | .0595 | -.2061 | .3105 | -.1261 | -.0570 | -.6206 | -.1040 |
| (87) | -.03 | .26 | -.08 | -.24 | -.04 | .04 | -.20 | .30 | -.12 | -.09 | -.56 | -.08 |
| A1 | .2047 | .0405 | -.2648 | -.0148 | .0655 | -.0153 | .3154 | -.1795 | -.0384 | -.1192 | -.0937 | -.5886 |
| (65) | .21 | .02 | -.26 | -.03 | .10 | -.02 | .30 | -.19 | -.07 | -.12 | -.17 | -.60 |

equation (56) as 0.53. This value of F agrees with that obtained from the best fit of the $G_{ab, cd}$ curves in Figs. 5, 6 and 7.

2. Sample B

Double resonance experiments were performed on all twelve lines of sample B. The signal heights of single and double resonance spectra and the width of the double resonance lines, $W^D$, when different from the single resonance lines, are listed in Table 6. The line width of each single resonance line is .50 $H_z$. The strength of the second rf is .076 $H_z$. The arrangement of the Table 6 is similar to Table 3. The $G_{ab, cd}$ for the twelve double resonance experiments are listed in Table 7. The arrangement of Table 7 is similar to Table 4. The experimental $G_{ab, cd}$ listed in Table 7 were computed using the corrected $I^{DR}$. The experimental points of $G_{ab, cd}$ are drawn in the Figs. 5, 6 and 7 as cross sign X. The $G_{ab, cd}$ have an experimental error of 15%. The F corresponding to the experimental points of $G_{ab, cd}$ may vary from .05 to .22. The best vertical line can be drawn through the experimental points of $G_{ab, cd}$ at F = .13.

Again we assumed TA = TB = TX, $C_{AB} = 1$, $C_{AX} = 0$ and $C_{BX} = 0$. The absolute values of TX and TD can be obtained by the best fit of the experimental $F_{ab, cd}$ and calculated $F_{ab, cd}$ for different values of TD and TX. In computing $F_{ab, cd}$, TD was varied from 15 to 21 seconds, TX was varied from 3 to 5 seconds, $C_{AB} = 1$, $C_{AX} = C_{BX} = 0$ and $H_2 = .076\ H_z$. The TD and TX obtained from the best fit of the experimental and calculated $F_{ab, cd}$ are 18 seconds and 4 seconds, respectively. The $F_{ab, cd}$ for all twelve double resonance experiments are listed in Table 8. The arrangement of Table 8 is similar to Table 5.

Table 6. $I^{SR}$, $I^{DR}$ and $W^{D}$ of Sample B

| | | X4 (51) | X3 (73) | X2 (62) | X1 (84) | B4 (42) | B3 (31) | B2 (86) | B1 (75) | A4 (43) | A2 (21) | A3 (87) | A1 (65) |
|---|---|---|---|---|---|---|---|---|---|---|---|---|---|
| X4 | $I^{DR}$ | | 3.5 | 4.4 | 6.3 | 5.4 | 4.8 | 4.0 | 6.2 | 7.0 | 5.1 | 5.2 | 4.6 |
| (51) | $W^{D}$ | | | | | | .55 | | .48 | | .54 | | .46 |
| X3 | $I^{DR}$ | 2.5 | | 4.4 | 5.4 | 5.3 | 6.5 | 3.4 | 3.8 | 5.1 | 5.5 | 5.4 | 3.7 |
| (73) | $W^{D}$ | | | | | | .55 | | .56 | .58 | | | |
| X2 | $I^{DR}$ | 2.7 | 3.6 | | 5.5 | 4.2 | 6.0 | 4.5 | 5.4 | 7.2 | 7.1 | 4.5 | 2.7 |
| (62) | $W^{D}$ | | | | | .51 | | .48 | | | .53 | | .58 |
| X1 | $I^{DR}$ | 2.9 | 3.5 | 4.3 | | 6.7 | 6.5 | 2.8 | 5.3 | 8.7 | 6.5 | 3.5 | 3.7 |
| (84) | $W^{D}$ | | | | | .48 | | .53 | .48 | .49 | | .54 | |
| B4 | $I^{DR}$ | 2.9 | 3.7 | 3.3 | 6.8 | | | 3.2 | 5.2 | 5.7 | 7.5 | 5.0 | 4.2 |
| (42) | $W^{D}$ | | | .58 | .54 | | | | .49 | .53 | | .47 | .48 |
| B3 | $I^{DR}$ | 2.1 | 4.7 | 4.7 | 6.8 | | | 3.8 | 5.0 | 8.5 | 5.0 | 5.3 | 4.0 |
| (31) | $W^{D}$ | .60 | .47 | .48 | | | | .48 | .47 | | .53 | .47 | .47 |
| B2 | $I^{DR}$ | 3.3 | 3.8 | 5.8 | 5.1 | 5.0 | 5.8 | | | 7.1 | 6.6 | 3.9 | 4.6 |
| (86) | $W^{D}$ | | .49 | .45 | .54 | | | | | | | .51 | .48 |
| B1 | $I^{DR}$ | 3.5 | 2.8 | 4.7 | 5.8 | 5.1 | 5.4 | | | 7.1 | 5.5 | 5.3 | 2.6 |
| (75) | $W^{D}$ | .51 | .55 | | | | | | | | .55 | .52 | .59 |
| A4 | $I^{DR}$ | 3.0 | 2.9 | 5.0 | 7.4 | 4.4 | 7.1 | 3.8 | 5.5 | | | 4.0 | 3.6 |
| (43) | $W^{D}$ | | | | .51 | | .53 | | | | | | |
| A2 | $I^{DR}$ | 2.1 | 3.6 | 5.3 | 6.5 | 6.1 | 4.2 | 4.0 | 5.0 | | | 4.4 | 3.2 |
| (21) | $W^{D}$ | .60 | | .53 | | .53 | .60 | .48 | | | | | |
| A3 | $I^{DR}$ | 3.3 | 4.7 | 4.6 | 4.9 | 5.3 | 5.8 | 2.9 | 5.9 | 6.2 | 5.6 | | |
| (87) | $W^{D}$ | | .44 | | .53 | | .54 | .53 | .51 | | .54 | | |
| A1 | $I^{DR}$ | 3.5 | 4.0 | 3.7 | 6.2 | 5.7 | 6.0 | 4.2 | 4.6 | 7.0 | 5.9 | | |
| (65) | $W^{D}$ | | | .53 | | | | | | | | | |
| | $I^{SR}$ | 3.1 | 3.7 | 4.6 | 6.3 | 5.3 | 6.1 | 3.6 | 5.2 | 7.1 | 6.4 | 4.7 | 3.8 |

Table 7. $G_{ab, cd}$ of Sample B

| | X4 (51) | X3 (73) | X2 (62) | X1 (84) | B4 (42) | B3 (31) | B2 (86) | B1 (75) | A4 (43) | A2 (21) | A3 (87) | A1 (65) |
|---|---|---|---|---|---|---|---|---|---|---|---|---|
| X4 | -1 | -.2867 | -.2851 | -.1723 | -.0553 | -.3575 | .0575 | .3558 | -.0666 | -.3688 | .0478 | .3461 |
| (51) | -1 | -.16 | -.13 | 0 | .06 | -.42 | .32 | .42 | -.03 | -.45 | .32 | .42 |
| X3 | -.2800 | -1 | -.1433 | -.2768 | .0664 | .3706 | -.0671 | -.3494 | -.3762 | -.0749 | .3441 | .0618 |
| (75) | -.39 | -1 | -.08 | -.29 | 0 | .33 | -.12 | -.35 | -.35 | -.29 | .31 | .06 |
| X2 | -.2764 | -.1423 | -1 | -.2772 | -.3581 | -.0687 | .3647 | .0655 | .0615 | .3510 | -.0734 | -.3726 |
| (62) | -.26 | -.06 | -1 | -.26 | -.38 | -.04 | .38 | .08 | .02 | .34 | -.08 | -.36 |
| X1 | -.1728 | -.2843 | -.2868 | -1 | .3525 | .0605 | -.3607 | -.0510 | .3430 | .0510 | -.3727 | -.0630 |
| (84) | -.13 | -.11 | -.15 | -1 | .46 | .15 | -.43 | -.09 | .43 | .04 | -.41 | -.07 |
| B4 | -.0569 | .0700 | -.3803 | .3619 | -1 | -.2500 | -.2578 | -.1231 | -.3411 | .4089 | -.0492 | .0856 |
| (42) | -.13 | 0 | -.38 | .36 | -1 | -.27 | -.24 | -.13 | -.33 | .42 | -.04 | .11 |
| B3 | -.3632 | .3855 | -.0719 | .0613 | -.2466 | -1 | -.1134 | -.2514 | .4071 | -.3464 | .0829 | -.0552 |
| (31) | -.37 | .37 | -.08 | .16 | -.29 | -1 | -.06 | -.24 | .39 | -.35 | .08 | -.06 |
| B2 | .0583 | -.0697 | .3814 | -.3647 | -.2539 | -.1132 | -1 | -.2412 | -.0535 | .0872 | -.3486 | .4103 |
| (86) | .16 | 0 | .34 | -.37 | -.16 | -.13 | -1 | -.29 | 0 | .08 | -.39 | .42 |
| B1 | .3703 | -.3722 | .0703 | -.0529 | -.1244 | -.2575 | -.2475 | -1 | .0824 | -.0508 | .4017 | -.3508 |
| (75) | .35 | -.35 | .04 | -.17 | -.09 | -.24 | -.30 | -1 | 0 | -.13 | .37 | -.39 |
| A4 | -.0683 | -.3980 | .0651 | .3507 | -.3397 | .4109 | -.0541 | .0811 | -1 | -.2494 | -.2513 | -.1160 |
| (43) | -.05 | -.39 | .16 | .35 | -.30 | .40 | .11 | .11 | -1 | -.30 | -.26 | -.09 |
| A2 | -.3758 | -.0781 | .3688 | .0518 | .4047 | -.3475 | .0877 | -.0498 | -.2479 | -.2479 | -.1179 | -.2553 |
| (21) | -.37 | -.06 | .36 | .06 | .38 | -.35 | .11 | -.08 | -.24 | -1 | -.11 | -.31 |
| A3 | .0494 | .3635 | -.0781 | -.3835 | -.0493 | .0842 | -.3547 | .3984 | -.2529 | -.1194 | -1 | -.2469 |
| (87) | .13 | .34 | 0 | -.37 | 0 | -.11 | -.37 | .37 | -.28 | -.13 | -1 | -.26 |
| A1 | .3528 | .0645 | -.3917 | -.0640 | .0807 | -.0554 | .4124 | -.3437 | -.1154 | -.2554 | -.2439 | -1 |
| (65) | .34 | .21 | -.39 | -.05 | .21 | -.05 | .45 | -.32 | -.03 | -.21 | -.29 | -1 |

Table 8. $F_{ab, cd}$ of Sample B

| | X4 (51) | X3 (73) | X2 (62) | X1 (84) | B4 (42) | B3 (31) | B2 (86) | B1 (75) | A4 (43) | A2 (21) | A3 (87) | A1 (65) |
|---|---|---|---|---|---|---|---|---|---|---|---|---|
| X4 | -.3771 | -.1081 | -.1075 | -.0650 | -.0209 | -.1348 | .0217 | .1342 | -.0251 | -.1391 | .0180 | .1305 |
| (51) | -.31 | -.05 | -.04 | 0 | .02 | -.13 | .10 | .13 | -.01 | -.14 | .10 | .13 |
| X3 | -.1260 | -.4498 | -.0645 | -.1245 | .0299 | .1667 | -.0302 | -.1572 | -.1706 | -.0337 | .1548 | .0278 |
| (75) | -.19 | -.49 | -.04 | -.14 | 0 | .16 | -.06 | -.17 | -.17 | -.14 | .15 | .03 |
| X2 | -.1385 | -.0713 | -.5010 | -.1389 | -.1794 | -.0344 | .1827 | .0328 | .0308 | .1758 | -.0368 | -.1867 |
| (62) | -.13 | -.03 | -.50 | -.13 | -.19 | -.02 | .19 | .04 | .01 | .17 | -.04 | -.18 |
| X1 | -.0972 | -.1600 | -.1614 | -.5627 | .1984 | .0341 | -.2030 | -.0287 | .1930 | .0287 | -.2097 | -.0354 |
| (84) | -.06 | -.05 | -.07 | -.46 | .21 | .07 | -.20 | -.04 | .20 | .02 | -.19 | -.03 |
| B4 | -.0277 | .0341 | -.1852 | .1762 | -.4869 | -.1217 | -.1255 | -.0599 | -.1661 | .1991 | -.0240 | .0417 |
| (42) | -.06 | 0 | -.17 | .16 | -.45 | -.12 | -.11 | -.06 | -.15 | .19 | -.02 | .05 |
| B3 | -.1880 | .1996 | -.0373 | .0317 | -.1277 | -.5178 | -.0587 | -.1302 | .2108 | -.1793 | .0429 | -.0286 |
| (31) | -.19 | .19 | -.04 | .08 | -.15 | -.51 | -.03 | -.12 | .20 | -.18 | .04 | -.03 |
| B2 | .0229 | -.0273 | .1495 | -.1429 | -.0995 | -.0444 | -.3919 | -.0945 | -.0210 | .0342 | -.1366 | .1608 |
| (86) | .06 | 0 | .13 | -.14 | -.06 | -.05 | -.38 | -.11 | 0 | .03 | -.15 | .16 |
| B1 | .1704 | -.1713 | .0323 | -.0243 | -.0572 | -.1185 | -.1139 | -.4602 | .0379 | -.0234 | .1848 | -.1614 |
| (75) | .16 | -.16 | .02 | -.08 | -.04 | -.11 | -.14 | -.46 | 0 | -.062 | .17 | -.18 |
| A4 | -.0370 | -.2156 | .0353 | .1900 | -.1840 | .2226 | -.0293 | .0440 | -.5417 | -.1351 | -.1361 | -.0629 |
| (43) | -.03 | -.22 | .09 | .20 | -.17 | .23 | .06 | .06 | -.57 | -.17 | -.15 | -.05 |
| A2 | -.1887 | -.0392 | .1852 | .0260 | .2032 | -.1744 | .0440 | -.0250 | -.1244 | -.5020 | -.0592 | -.1282 |
| (21) | -.19 | -.03 | .19 | .03 | .20 | -.18 | .06 | -.04 | -.12 | -.51 | -.06 | -.16 |
| A3 | .0211 | .1557 | -.0335 | -.1643 | -.0211 | .0361 | -.1519 | .1707 | -.1083 | -.0512 | -.4283 | -.1058 |
| (87) | .06 | .16 | 0 | -.17 | 0 | -.05 | -.17 | .17 | -.13 | -.06 | -.46 | -.12 |
| A1 | .1325 | .0242 | -.1471 | -.0240 | .0318 | -.0208 | .1549 | -.1291 | -.0433 | -.0959 | -.0916 | -.3755 |
| (65) | .13 | .08 | -.15 | -.02 | .08 | -.02 | .17 | -.12 | -.01 | -.08 | -.11 | -.38 |

The experimental values of $F_{ab,ab}$ are obtained from the average of equations (36) and (37). In general the experimental and calculated $F_{ab,cd}$ in Table 8 agree within experimental error of 10%. Since the absolute TD and TX can be obtained from the above comparison, F can be obtained from equation (56) as .18. This value of F falls within the range of the $G_{ab,cd}$ curves in Figs. 5, 6 and 7. The range on Figs. 5, 6 and 7 is large because the experimental error is large and most of the $G_{ab,cd}$ curves in this region have a small slope.

3. Discussion

From the above results, sample A has 53% intramolecular dipolar interaction with TD = 18 seconds and TX = 20 seconds and sample B has 18% intramolecular dipolar interaction with TD = 18 seconds and TX = 4 seconds. Because the make-up of the two sample differ only by sample B having dissolved $O_2$, it is reasonable to assume that TD is the same for both samples. However, sample B has a stronger intermolecular dipolar interaction because of the oxygen molecules. This shows up in a lower value of TX.

The weak double resonance experiment is a straightforward and simple technique for studying relaxation processes in three spin systems. The features of double resonance spectra can be interpreted from the density matrix formalism.

The advantage of using $G_{ab,cd}$ is that it is independent of small frequency off sets and the strength of $H_2$, and also requires only relative relaxation times for interpretation. The disadvantage of using $G_{ab,cd}$ is that it has a larger experimental error than $F_{ab,cd}$. Also, the absolute relaxation parameters can not be obtained from the $G_{ab,cd}$. The plots of $G_{ab,cd}$ versus F serve a similar function for estimating the relative contribution of different relaxation processes as the strong double resonance experiments used by other investigators.[10] The reason that the strong double resonance experiments depend only on the relative contributions is that the experiments may be described by Bloch's approximation.[13] This can be seen in equation (10) of reference 10.

The experimental results of three spin systems are sensitive to the relaxation mechanisms. The studies in two spin systems in reference 6 showed the same kind of sensitivity to the relaxation mechanisms. In addition, the three spin systems have a great variety of features in their double resonance spectra. Hence, this allows the study of interesting relations like the symmetry properties and summation rule of the $G_{ab,cd}$ and $F_{ab,cd}$. The symmetry properties were developed for the special case of weak coupling and simplified relaxation mechanism. It is interesting that these relations for the $G_{ab,cd}$ hold approximately for the tightly coupled three spin systems.

The two spin system can not be used to study anisotropic reorientation[23] because the Overhauser effect does not depend on the anisotropic reorientation. However, for the three spin system, the Overhauser effect in principle does depend on the anisotropic reorientation.[6] Hence, it may be interesting to study the effect of anisotropic reorientation on the double resonance spectra of three spin systems.

# APPENDIX

*Reprinted from:*

THE JOURNAL OF CHEMICAL PHYSICS VOLUME 54, NUMBER 4 15 FEBRUARY 1971

# Nuclear Magnetic Double Resonance in Chemically Exchanging Systems*

PING P. YANG AND SIDNEY L. GORDON

*School of Chemistry, Georgia Institute of Technology, Atlanta, Georgia 30332*

(Received 6 August 1970)

A density matrix description of nuclear magnetic double resonance on chemically exchanging systems is developed using a double resonance basis set. The chemical exchange coefficients have many properties analogous to the relaxation coefficients. This allows the density matrix computation to be expressed in terms of a symmetric array. The solutions can then be obtained in terms of an eigenvalue procedure. This procedure is more efficient than standard Gauss–Jordan reduction and automatically takes into account the constraints introduced by the summation properties of the relaxation and chemical exchange coefficients and by the symmetry of the spin system. The formalism is illustrated by self-exchange in the $AB_2$ system, 2,2,2-trichloroethanol. Comparison of theoretical and experimental double resonance spectra allow the determination of the chemical exchange lifetime and the relaxation parameters even when the exchange rates are slow compared with the experimental linewidths.

## I. INTRODUCTION

In nuclear magnetic double resonance, the NMR spectrum is swept by a weak observing rf, $\mathbf{H}_1$, while the spin system is simultaneously irradiated by a second strong rf, $\mathbf{H}_2$.[1,2a] The strong rf produces population changes which show up as intensity changes in the recorded spectrum. In addition, double resonance splittings appear when the strength of the strong rf is comparable to the linewidths.

Nuclear magnetic double resonance has proven to be a valuable technique for studying relaxation processes in coupled spin systems.[2a] Chemical exchange of nuclear spins has many features similar to relaxation, and one would expect that an analysis of the double resonance spectrum of a chemically exchanging system would provide information on both the chemical exchange processes and the relaxation mechanisms.

In this paper, a formalism for double resonance on chemically exchanging systems is developed by combining the relaxation formalism of Redfield[3] with the chemical exchange formalism of Alexander.[4] The formalism is developed explicitly for intermolecular chemical exchange. Intramolecular conformer changes, however, are just a special case of intermolecular exchange.[5]

Double resonance techniques have been used often to study chemical exchange processes by monitoring transfer of saturation.[6–9] This paper differs from the others in that chemical exchange is incorporated into a density matrix double resonance formalism.[2a,10]

The formalism is developed using a double resonance basis set.[2a,10] This provides a formulation which is exact for all values of irradiation strengths.

The exchange coefficients have many properties analogous to the relaxation coefficients. This allows the double resonance calculation to be expressed in terms of a symmetric array. The solutions can then be obtained in terms of an eigenvalue procedure. This procedure appears to be more efficient on a computer than standard Gauss–Jordan reduction.

The formalism is illustrated by the $AB_2$ system, 2,2,2-trichloroethanol. In addition to line broadening, the chemical exchange tends to redistribute the population changes caused by the strong rf field. Hence, the nuclear Overhauser effect[2a] depends on the chemical exchange rates. The chemical exchange lifetimes and relaxation parameters may be measured by fitting experimental and theoretical double resonance spectra. This is possible even when the exchange rates are slow compared with the experimental linewidths.

## II. INSTRUMENTATION AND SAMPLES

Frequency sweep double resonance spectra were obtained at 100 MHz with a JEOL 4H-100 NMR spectrometer. This instrument uses an internal lock modulation frequency of 4 kHz. The strong rf, $\mathbf{H}_2$, was obtained from a General Radio 1164-A synthesizer. The lowest frequency which can be directly obtained from the GR synthesizer is 0.1 MHz. The required audio signal was obtained from the synthesizer by mixing the 5-MHz synthesizer reference signal (J108 on the synthesizer) with the synthesizer output signal, by using a Hewlett–Packard 1951A mixer. The $\mathbf{H}_2$ signal was amplified using a GR 1206-B unit amplifier and attenuated by a HP 250-D attenuator. Precision double resonance experiments are difficult on compounds with short relaxation times because of the large response due to $\mathbf{H}_2$. Interference from the strong signal at $\omega_2$ was considerably reduced by placing a Spectral Dynamics SD101B tracking filter with a 2.0-Hz bandwidth before the audio phase detector.

The samples were prepared in standard 5-mm-o.d. NMR tubes fitted with standard taper joints and ground glass stoppers. The 2,2,2-trichloroethanol was obtained from Aldrich and was distilled before use. It was found that the hydroxyl exchange rate could be reduced to extremely low levels by simply shaking the substance with Fisher type 5A molecular sieves before use. The experiments for Fig. 2 were on a $CS_2$ solution containing about 5% by volume of alcohol, 5% by volume of tetramethylsilane for the lock signal, and a drop of cyclohexane to monitor the receiver amplification. The experiments for Fig. 3 were on a sample of approximately the same composition (as measured by the chemical shift) but to which a few drops of $CS_2$ saturated with HCl were added to increase the exchange rate of the hydroxyl proton.

## III. FORMALISM

### A. Density Matrix Equations

The development of Sec. III will assume an exchange process involving only one nucleus and one type of molecule (self-exchange). The extension to one nucleus exchanging between two types of molecules is treated in the Appendix. The extension of the formalism to exchange of several nuclei may be done in a straightforward manner.

In nuclear magnetic double resonance, the spin system is simultaneously irradiated by a strong saturating rf field $\mathbf{H}_2$ at angular frequency $-\omega_2$ and a weak observing rf field at angular frequency $-\omega_1$. It is assumed that double resonance on a chemically exchanging spin system is described in the rotating frame by

$$(d\tilde{\sigma}/dt)+i[\mathcal{H}_0^R,\tilde{\sigma}]+i[D_{1+},\tilde{\sigma}]\exp(i\omega' t)+i[D_{1-},\tilde{\sigma}]\times\exp(-i\omega' t)+\Gamma(\tilde{\sigma}-\sigma_0)+E(\tilde{\sigma})=0. \quad (1)$$

In Eq. (1), $\tilde{\sigma}$ is the spin density matrix in the rotating frame, and $\sigma_0$ is the equilibrium value of the spin density matrix with no rf fields. $\mathcal{H}_0^R$ is the time-independent part of the Hamiltonian and is given by[1,2a]

$$\mathcal{H}_0^R=2\pi\{\sum_i A_i\mathcal{F}_z(i)+\sum J_{ij}\mathcal{F}(i)\cdot\mathcal{F}(j)\}+D_{2+}+D_{2-}. \quad (2)$$

In Eqs. (1) and (2), $A_i=-v_{0i}+(\omega_2/2\pi)$, $\mathcal{F}(i)$ is the spin vector for the magnetically equivalent set $i$,

$$D_{k\pm}=-\pi\sum_i v_{ki}\mathcal{F}_\pm(i), \qquad k=1,2,$$

$$v_{ki}=\gamma_i H_k/(2\pi), \qquad k=0,1,2,$$

$$\omega'=\omega_1-\omega_2,$$

and the remaining symbols have their usual meaning.[1,2a,2b] In this paper, $\sigma_0$ will be assumed to be adequately described by

$$\sigma_0=(1/N)+2\pi q\sum_i v_{0i}\mathcal{F}_z(i), \quad (3)$$

where $N$ is the number of spin states and $q=\hbar/(NkT)$.

In the following, the kets $|\alpha\rangle$, $|\alpha'\rangle$, $|\beta\rangle$, $|\beta'\rangle$, $\cdots$, etc., will denote the basis in which $\mathcal{H}_0^R$ is diagonal,[1,2,10] such that

$$\mathcal{H}_0^R|\alpha\rangle=E_\alpha|\alpha\rangle. \quad (4)$$

The relaxation of the spin system is described by $\Gamma(\tilde{\sigma}-\sigma_0)$, where

$$\langle\alpha|\Gamma(\tilde{\sigma}-\sigma_0)|\beta\rangle=-\sum_{\alpha'\beta'}R_{\alpha\beta\alpha'\beta'}(\langle\alpha'|\tilde{\sigma}|\beta'\rangle-\langle\alpha'|\sigma_0|\beta'\rangle), \quad (5)$$

and the $R_{\alpha\beta\alpha'\beta'}$ elements are given by the Redfield formulation.[2a,8] The $R_{\alpha\beta\alpha'\beta'}$ relaxation elements satisfy the important relations[2a,10]

$$\sum_\alpha R_{\alpha\alpha\alpha'\beta'}=0 \quad (6)$$

and

$$R_{\alpha\beta\alpha'\beta'}=R_{\alpha'\beta'\alpha\beta}=R_{\beta\alpha\beta'\alpha'}. \quad (7)$$

The chemical exchange is described by $E(\tilde{\sigma})$, where $E(\tilde{\sigma})$ was given by Alexander[4] as

$$E(\tilde{\sigma})=\tau^{-1}[\Omega' P\tilde{\sigma}\cdot\tilde{\sigma}' P-\tilde{\sigma}]. \quad (8)$$

In Eq. (8) $\tau$ is average time between chemical exchanges, $\tilde{\sigma}'$ is the density matrix for a second molecule, $P$ is a permutation operator describing the chemical exchange, and $\Omega'$ means trace over the spin states of the second molecule.

The steady state density matrix equations are derived by taking components of (1) with respect to the double resonance basis, and substituting (2), (3), (5), and (8). It is assumed that

$$\langle\alpha|\tilde{\sigma}|\beta\rangle=\langle\alpha|\sigma_0|\beta\rangle+\langle\alpha|\chi|\beta\rangle+\langle\alpha|\eta|\beta\rangle, \quad (9)$$

where $\chi$ is due to $\mathbf{H}_2$ and $\eta$ is due to $\mathbf{H}_1$. In addition, it is assumed that the off-diagonal elements of $\langle\alpha|\eta|\beta\rangle$ are given by

$$\langle\alpha|\eta|\beta\rangle=\langle\alpha|\eta^+|\beta\rangle\exp(i\omega' t)+\langle\alpha|\eta^-|\beta\rangle\times\exp(-i\omega' t), \quad (10)$$

where $\langle\alpha|\eta^+|\beta\rangle=\langle\beta|\eta^-|\alpha\rangle^*$. Then, to first order in $\omega_1/kT$ and $(2\pi v_1)/R_{\alpha\beta\alpha'\beta'}$, $\langle\alpha|\chi|\beta\rangle$ and $\langle\alpha|\eta^-|\beta\rangle$ satisfy the equations

$$i\omega_{\alpha\beta}\langle\alpha|\chi|\beta\rangle-\sum_{\alpha'\beta'}R_{\alpha\beta\alpha'\beta'}\langle\alpha'|\chi|\beta'\rangle-\sum_{\alpha'\beta'}E_{\alpha\beta\alpha'\beta'}\langle\alpha'|\chi|\beta'\rangle=-i2\pi q\omega_{\alpha\beta}\times\langle\alpha|\sum_i v_{0i}\mathcal{F}_z(i)|\beta\rangle, \quad (11)$$

$$i(\omega_{\alpha\beta}-\omega')\langle\alpha|\eta^-|\beta\rangle-\sum_{\alpha'\beta'}R_{\alpha\beta\alpha'\beta'}\langle\alpha'|\eta^-|\beta'\rangle-\sum_{\alpha'\beta'}E_{\alpha\beta\alpha'\beta'}\langle\alpha'|\eta^-|\beta'\rangle=i\pi v_1\langle\alpha|[\mathcal{F}_-,2\pi q\sum_i v_{0i}\mathcal{F}_z(i)+\chi]|\beta\rangle, \quad (12)$$

and

$$\sum_\alpha\langle\alpha|\chi|\alpha\rangle=\sum_\alpha\langle\alpha|\eta^-|\alpha\rangle=0, \quad (13)$$

where $\omega_{\alpha\beta}=E_\alpha-E_\beta$. These equations are the standard double resonance density matrix equations[2a,10] except for the additions of the exchange terms, described by the elements $E_{\alpha\beta\alpha'\beta'}$. The signal detected at $\omega_1$ is proportional to $S$, where

$$S=\mathrm{Im}\sum_{\alpha,\beta}\langle\alpha|\eta^-|\beta\rangle\langle\beta|\mathcal{F}_+|\alpha\rangle, \quad (14)$$

and Im means the imaginary part.

### B. Exchange Coefficients

The exchange coefficients are given by

$$E_{\alpha\beta\alpha'\beta'}=\tau^{-1}[(\mathrm{Tr}B^{\alpha\alpha'}B^{\beta'\beta}/N_n)+(\mathrm{Tr}B^{\alpha\beta}B^{\beta'\alpha'}/N_e)-\delta_{\alpha\alpha'}\delta_{\beta\beta'}], \quad (15)$$

where the matrix $B^{\alpha\beta}$ is defined by

$$(B^{\alpha\beta})_{ab}=\sum_{\mathfrak{f}} C_{\mathfrak{f}a}{}^{\alpha}C_{\mathfrak{f}b}{}^{\beta}, \quad (16)$$

and Tr stands for trace. In Eq. (16), $C_{\mathfrak{f}a}{}^{\alpha}$ is an expansion coefficient for $|\alpha\rangle$, defined by

$$|\alpha\rangle=\sum_{\mathfrak{f}a} C_{\mathfrak{f}a}{}^{\alpha}|\mathfrak{f}\rangle|a\rangle, \quad (17)$$

where $|\mathfrak{f}\rangle$ is a member of a basis set for the exchanging nucleus, and $|a\rangle$ is a member of a basis set for the nonexchanging nuclei. $N_e$ is the dimension of $|\mathfrak{f}\rangle$, and $N_n$ is the dimension of $|a\rangle$. $\tau$ is the average lifetime of the exchanging nucleus on one molecule. It is seen from their definition in Eq. (16) that the $B^{\alpha\beta}$ matrices satisfy the relation $(B^{\alpha\beta})_{ab}=(B^{\beta\alpha})_{ba}$. The exchange coefficients transform like 4th-rank tensors with respect to a change of basis. Thus, if $U_{\alpha^t\alpha}=\langle\alpha^t|\alpha\rangle$,

$$E_{\alpha^t\beta^t\gamma^t\delta^t}=\sum_{\alpha\beta\gamma\delta} U_{\alpha^t\alpha}U_{\beta^t\beta}U_{\gamma^t\gamma}U_{\delta^t\delta}E_{\alpha\beta\gamma\delta}. \quad (18)$$

Other useful properties which may be proven from the definition, Eq. (15), are

$$E_{\alpha\beta\alpha'\beta'}=E_{\beta\alpha\beta'\alpha'}=E_{\alpha'\beta'\alpha\beta}, \quad (19)$$

$$\sum_{\alpha} E_{\alpha\alpha\alpha'\beta'}=\tau^{-1}\delta_{\alpha'\beta'}, \quad (20)$$

$$\sum_{\alpha'\beta'} E_{\alpha\beta\alpha'\beta'}\langle\alpha'|\sum_i v_{0i}\mathfrak{F}_z(i)|\beta'\rangle=0, \quad (21)$$

and

$$\sum_{\alpha\subset\Gamma} E_{\alpha\alpha\alpha'\beta'}=(N^{\Gamma}/N)\tau^{-1}\delta_{\alpha'\beta'}. \quad (22)$$

Equation (22) is obtained if the spin system has symmetry. Then $\Gamma$ represents one species, and the summation is over all states which belong to that species. $N^{\Gamma}$ is the dimension of the species $\Gamma$, and $N$ is the total number of spin states.

### C. Solution of Eq. (11) for No Relaxation

In order to understand the effects of chemical exchange, the solution of Eq. (11) will be examined in the limit of $R_{\alpha\beta\alpha'\beta'}\rightarrow 0$, i.e.,

$$i\omega_{\alpha\beta}\langle\alpha|\chi|\beta\rangle-\sum_{\alpha'\beta'} E_{\alpha\beta\alpha'\beta'}\langle\alpha'|\chi|\beta'\rangle=-i2\pi q\omega_{\alpha\beta}\langle\alpha|\sum_i v_{0i}\mathfrak{F}_z(i)|\beta\rangle. \quad (23)$$

Using Eq. (21), it is seen that an exact solution of Eq. (23) is

$$\chi=-2\pi q\sum_i v_{0i}\mathfrak{F}_z(i). \quad (24)$$

This solution corresponds to complete saturation of the spin system. Notice, however, that (24) is the solution of Eq. (23) even when $E_{\alpha\beta\alpha'\beta'}=0$. Physically, this occurs because Eq. (23) is an exact description and *every* transition is directly irradiated. Because there is no relaxation to oppose the effects of the rf field, every transition is saturated. That the chemical exchange does not oppose the saturation is no surprise; this may be inferred directly from the Alexander operator expression (8). Therefore, relaxation must be included in an analysis which allows saturation. This is true even though chemical exchange by itself may be adequate in formalisms which neglect saturation.[11]

### D. Numerical Solution

When one attempts to quantitatively describe double resonance spectra with chemical exchange, one has the practical difficulty that the chemical exchange may couple the density matrix elements strongly. Then, the widely used Bloch approximation and simple line approximation are not adequate.[2a] We have found that the speed of a computation is improved by at least a factor of 3 by using a diagonalization procedure. Besides the advantage in computer time, this procedure automatically accounts for the constraints introduced by relations (6), (20), (21), and molecular symmetry coupled with (22). The diagonalization procedure we used will be discussed in detail in Sec. III.D.[12]

The real and imaginary parts of Eqs. (11) and (12) may be written in terms of a symmetric array by a simple change of variables. With this in mind, it is convenient to designate the diagonal elements, and the real and imaginary parts of the off-diagonal elements as follows:

$$\langle\alpha|\chi|\alpha\rangle=\langle\alpha|\chi_0|\beta\rangle, \quad (25)$$

$$\langle\alpha|\chi|\beta\rangle=\langle\alpha|\chi_1|\beta\rangle+i\langle\alpha|\chi_2|\beta\rangle, \quad (26)$$

and

$$\langle\alpha|\eta^-|\beta\rangle=\langle\alpha|\eta_1^-|\beta\rangle+i\langle\alpha|\eta_2^-|\beta\rangle. \quad (27)$$

Because $\tilde{\sigma}$ is Hermitian,

$$\langle\alpha|\chi_1|\beta\rangle=\langle\beta|\chi_1|\alpha\rangle$$

and

$$\langle\alpha|\chi_2|\beta\rangle=-\langle\beta|\chi_2|\alpha\rangle. \quad (28)$$

Only the elements $\langle\alpha|\chi_\xi|\beta\rangle$ with $\alpha\leq\beta$ need be computed because of relations (28). The indices of $\langle\alpha|\chi_\xi|\beta\rangle$ will be considered to define an ordered triplet $\xi\alpha\beta$. The $\xi\alpha\beta$ triplets will be ordered in a linear array by successively stepping each index through its range of values, starting with $\xi$. Thus, $\xi$ is incremented from 0 to 2. When $\xi$ equals 0, the pair $\alpha\beta$ is stepped through the sequence 11, 22, $\cdots$, $NN$, where $N$ is the number of spin states. For $\xi$ equal to 1 or 2, the pair $\alpha\beta$ is stepped through the sequence 12, 13, $\cdots$, $1N$, 23, $\cdots$, $2N$, $\cdots$, $N-1N$.

Let $k$ denote the position of the triplet $\xi\alpha\beta$ in the sequence defined above. This defines a one-to-one

TABLE I. $A_{kk'}$.

| $\xi$ | $\xi'$ | $A_{kk'}$ |
|---|---|---|
| 0 | 0 | $2(R_{\alpha\alpha\alpha'\alpha'}+E_{\alpha\alpha\alpha'\alpha'})$ |
| 0 | 1 | $2(R_{\alpha\alpha\alpha'\beta'}+E_{\alpha\alpha\alpha'\beta'})$ |
| 0 | 2 | 0 |
| 1 | 1 | $(R_{\alpha\beta\alpha'\beta'}+R_{\alpha\beta\beta'\alpha'})+(E_{\alpha\beta\alpha'\beta'}+E_{\alpha\beta\beta'\alpha'})$ |
| 1 | 2 | $\omega_{\alpha\beta}\delta_{\alpha\alpha'}\delta_{\beta\beta'}$ |
| 2 | 2 | $-(R_{\alpha\beta\alpha'\beta'}-R_{\alpha\beta\beta'\alpha'})-(E_{\alpha\beta\alpha'\beta'}-E_{\alpha\beta\beta'\alpha'})$ |

mapping of the ordered triplet $\xi\alpha\beta$ onto the single index $k$. Therefore, $\xi\alpha\beta$ is a function of $k$ and may be written $\xi\alpha\beta(k)$. Similarly, $k$ is a function of $\xi\alpha\beta$, and may be written as $k(\xi\alpha\beta)$. The functional dependence of $k$ on $\xi\alpha\beta$ depends upon the spin system and must be derived by the procedure described above. In general, however, $\xi\alpha\beta(k)=0kk$ for $1\leq k\leq N$, where $N$ is the number of spin states. In the following, the second index or second triplet of indices will be primed, and the functional dependence of $k$ on $\xi\alpha\beta$ will be implied. Therefore, $A_{k(\xi\alpha\beta)k'(\xi'\alpha'\beta')}$ will be written simply as $A_{kk'}$ and $R_{\alpha\beta(k)\alpha'\beta'(k')}$ will be written as $R_{\alpha\beta\alpha'\beta'}$. With these conventions, Eq. (11) will be compactly written as

$$A\mathbf{X}=K, \tag{29}$$

where

$$\mathbf{X}_k=\tfrac{1}{2}\langle\alpha\mid\chi_0\mid\alpha\rangle \text{ for } 1\leq k\leq N$$
$$=\langle\alpha\mid\chi_\xi\mid\beta\rangle \text{ for } k>N,$$
$$K_k=-2\pi q\omega_{\alpha\beta}\langle\alpha\mid\sum_i v_{0i}\mathfrak{F}_z(i)\mid\beta\rangle\delta_{\xi 2},$$

and $A$ is a symmetric matrix whose elements $A_{kk'}$ are given in Table I for $k\leq k'$. The diagonal elements are multiplied by 1/2 in order to make $A$ symmetric. It is seen that $A_{kk'}=A_{k'k}$ by using Relations (7) and (19).

The form of $A$ is illustrated for an $AB$ system in Fig. 1. The upper-left-hand block, bounded by $A_{11}$, $A_{14}$, $A_{44}$, and $A_{41}$ represents the interactions between the diagonal elements of $\chi$. The next block along the diagonal, bounded by $A_{55}$, $A_{5,10}$, $A_{10,10}$, and $A_{10,5}$, represents the interactions between the real parts of the off-diagonal elements of $\chi$. The lowest block on the diagonal, bounded by $A_{11,11}$, $A_{11,16}$, $A_{16,16}$, and $A_{16,11}$, represents the interactions between the imaginary parts of the off-diagonal elements of $\chi$. It is seen that there are no elements connecting the blocks for the diagonal elements and the imaginary parts of the off-diagonal elements.

In practice, many of the off-diagonal elements of $\chi$ may be approximated using the Bloch approximation.[2,13] For each off-diagonal element of $\chi$ for which

$$|\omega_{\alpha\beta}|\gg|\langle\alpha\mid\Gamma(\chi)\mid\beta\rangle+\langle\alpha\mid E(\chi)\mid\beta\rangle|, \tag{30}$$

$$\langle\alpha\mid\chi\mid\beta\rangle\sim-2\pi q\langle\alpha\mid\sum_i v_{0i}\mathfrak{F}_z(i)\mid\beta\rangle. \tag{31}$$

It is obvious that the resulting $A$ matrix is still symmetric. In fact, the reduced $A$ matrix is obtained from the $A$ array for a complete calculation by simply deleting the rows and columns corresponding to the approximated elements. We have found it convenient to set up the complete $A$ array and then to delete the rows and columns by an array transfer procedure before using the diagonalization procedure. When $A$ is reduced, the elements of $K$ corresponding to the approximated $\mathbf{X}_k$ are also deleted. The remaining elements of the reduced $K$ array are then computed in an obvious manner.

Since $A$ is real and symmetric, it is diagonalized by an orthogonal transformation $U$, where

$$U^{-1}AU=\mathrm{diag}(a_1,a_2,\cdots,a_n). \tag{32}$$

Using Eqs. (6) and (20), it is seen that a general eigenvector of $A$ is $U^1$, where

$$U_k{}^1=(1/N^{1/2}),\qquad 1\leq k\leq N$$
$$=0,\ k>N,$$

and

$$a_1=2/\tau.$$

If the spin system has symmetry, and if a relaxation mechanism such as uncorrelated external random field is used, then $R_{\alpha\beta\alpha'\beta'}=0$ unless $|\alpha\rangle$, $|\beta\rangle$, $|\alpha'\rangle$ and $|\beta'\rangle$ belong to the same species.[14] If there are $p$ irreducible representations, then, using (22), it may be shown that the eigenvalue 0 occurs $p-1$ times.

The general solution of Eq. (29) is

$$\mathbf{X}_k=\sum_{l\neq 1}a_l{}^{-1}U_{kl}\sum_{m=1}^{n}U_{ml}K_m. \tag{33}$$

The sum over $l$ in Eq. (33) does not include $l=1$ and is

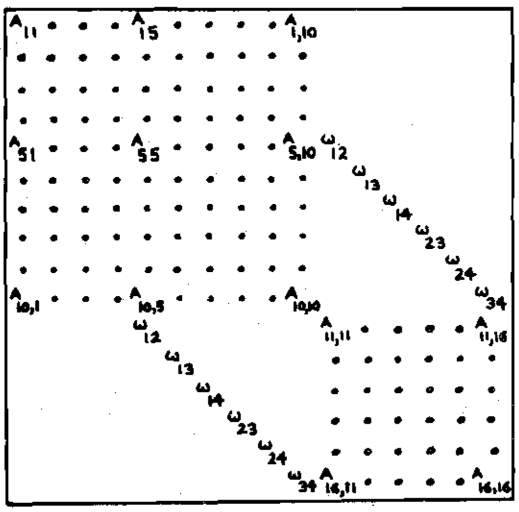


FIG. 1. Schematic form of $A$ for $AB$ system. The elements which have no symbol are identically zero.

restricted to values of $l$ for which $a_l \neq 0$. It is useful to note, however, that if desired, these terms could be included with arbitrary values for the corresponding $a_l^{-1}$. In this case, the off-diagonal elements of $\chi$ would be unaffected, and a constant would be added to each diagonal element of $\chi$. This would not affect the computed spectra, however, because only the *differences* between diagonal elements appear in subsequent computations. This feature can be useful in computer computations on systems with approximate symmetry because the calculation is guaranteed to be stable.

The computation of $\eta^-$ has the added feature that $\langle\alpha \mid \eta^- \mid \beta\rangle$ and $\langle\beta \mid \eta^- \mid \alpha\rangle$ are not simply related and can both contribute to the spectrum. Thus, the ordering of the $\xi\alpha\beta$ triplets must be slightly modified.

In analogy to the computation of $\chi$, $\xi$ is incremented first, but now through only the values 1 and 2. For $\xi$ equal to 1 or 2, the pair $\alpha\beta$ is stepped through the sequence 12, 21, 13, 31, $\cdots$, $1N$, $N1$, $\cdots$, 23, 32, $\cdots$, $2N$, $N2$, $\cdots$, $N-1N$, $NN-1$. Let $k$ once again denote the position of the triplet in the sequence just defined. Similarly to the computation of $\chi$, this defines a one-to-one mapping of the ordered triplet $\xi\alpha\beta$ onto the single index $k$.

With these conventions, Eq. (12) may be written

$$GH = L, \tag{34}$$

where

$$H_k = \langle\alpha \mid \eta_\xi^- \mid \beta\rangle,$$

$$L_k = \pi v_1 \langle\alpha \mid [\mathfrak{F}_-, \mathrm{Im}\chi] \mid \beta\rangle \delta_{\xi 1} + \pi v_1 \langle\alpha \mid [\mathfrak{F}_-, \mathrm{Re}\chi + 2\pi q \sum_i v_{0i} \mathfrak{F}_z(i)] \mid \beta\rangle \delta_{\xi 2},$$

and $G$ is a symmetric matrix whose elements $G_{kk'}$ are given in Table II for $k<k'$. The form of the $G$ matrix is similar to the $A$ matrix with the first $N$ rows and columns delected. In practice, the $G$ matrix may be greatly reduced. If transition $\gamma\delta$ is irradiated, then $\langle\alpha \mid \eta^- \mid \beta\rangle \sim 0$ for all transitions $\alpha\beta$ not overlapping with $\gamma\delta$. As with $A$, the reduced $G$ array is obtained from the complete $G$ array by simply deleting rows and columns corresponding to the approximated elements. The reduced $G$ matrix is still symmetric. As with $A$, we have found it convenient to set up the complete $G$ array and then to delete the rows and columns by an array transfer procedure before using the diagonalization procedure. In this way, one can optimize the computation for different segments of a spectrum and effectively obtain an exact computation using a small

TABLE II. $G_{kk'}$.

| $\xi$ | $\xi'$ | $G_{kk'}$ |
|---|---|---|
| 1 | 1 | $R_{\alpha\beta\alpha'\beta'} + E_{\alpha\beta\alpha'\beta'}$ |
| 1 | 2 | $(\omega_{\alpha\beta} - \omega')\delta_{\alpha\alpha'}\delta_{\beta\beta'}$ |
| 2 | 2 | $-R_{\alpha\beta\alpha'\beta'} - E_{\alpha\beta\alpha'\beta'}$ |

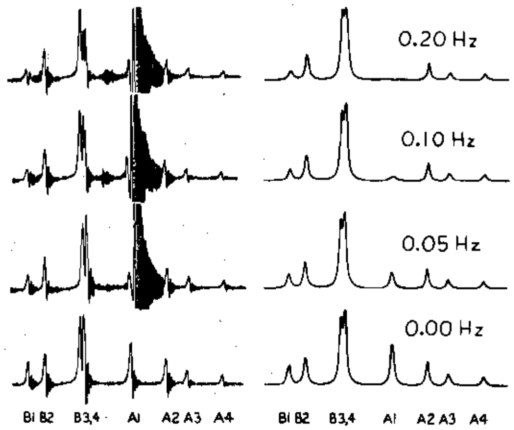


FIG. 2. Experimental and theoretical double resonance spectra. Values of $v_1$ are given on theoretical traces. Theoretical spectra computed with $\tau = 4$ sec, $T_A = T_B = 88$ sec, and $\lambda = 0.2$ Hz.

number of unknowns. The reduced $L$ array is obtained by simply deleting the elements corresponding to the approximated $H_k$. Defining $V$ by

$$V^{-1}GV = \mathrm{diag}(g_1, g_2, \cdots, g_n), \tag{35}$$

it is seen that

$$H_k = \sum_l g_l^{-1} V_{kl} \sum_m V_{ml} L_m. \tag{36}$$

The inhomogeneity of $H_0$ affects double resonance spectra in a complicated manner.[15] In this paper, the field inhomogeneity will be accounted for in an empirical manner by replacing all elements of the form $R_{\alpha\beta\alpha\beta} + E_{\alpha\beta\alpha\beta}$ by $R_{\alpha\beta\alpha\beta} + E_{\alpha\beta\alpha\beta} - \lambda$ when computing the $G$ array. The parameter $\lambda$ measures the contribution of field inhomogeneity to the half-width. This technique essentially produces Lorentzian line shapes with an inhomogeneity contribution of $\lambda$ to the half-width of the lines.

## IV. EXAMPLE: 2,2,2-TRICHLOROETHANOL

In Sec. IV, theory is compared with experiment for the $AB_2$ system 2,2,2-trichloroethanol. In this material, the hydroxyl proton undergoes acid or base catalyzed chemical exchange.

Experimental and theoretical frequency sweep double resonance spectra for 2,2,2-trichloroethanol are compared in Figs. 2 and 3. The bottom trace in each figure is a single resonance spectrum; the upper traces are double resonance spectra. The spectra were recorded with $\omega_1/2\pi$ decreasing from left to right at a sweep rate of 9 Hz/min. The hydroxyl resonances are labeled $A1$ to $A4$, and the methylene resonances are labeled B1 to $B4$. Line $A2$ corresponds to the antisymmetric transition.

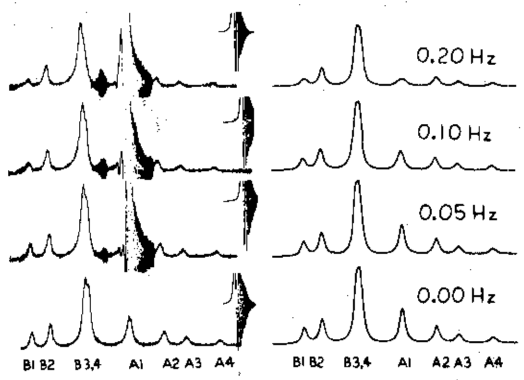


FIG. 3. Experimental and theoretical double resonance spectra. Values of $v_2$ are given on theoretical traces. Theoretical spectra computed with $\tau=0.5$ sec, $T_A=T_B=7$ sec, and $\lambda=0.2$ Hz.

The spectra in Fig. 2 were obtained using a 5% by volume solution of the alcohol in $CS_2$. The sample also contained 5% by volume of tetramethyl silane for the internal lock and a drop of cyclohexane to monitor the field inhomogeneity and to test for receiver saturation due to the strong irradiation. The chemical shift and coupling constant were determined to be 15.0±0.1 and 7.0±0.1 Hz, respectively, by fitting the experimental and computed spectra.

The spectra in Fig. 3 were obtained with a sample of approximately the same composition as that used for Fig. 2, but with a trace of HCl added. The increased exchange rate of the hydroxyl proton is apparent from the increased linewidths. The chemical shift for this sample was 14.0±0.1 Hz, and the coupling constant remained 7.0±0.1 Hz. The feature in the upper-right-hand corner of each experimental trace in Fig. 3 is the cyclohexane resonance.

The double resonance spectra were obtained by irradiating $A1$ with the strong rf field, $\mathbf{H}_2$. Irradiation of this line gave the most pronounced intensity changes. The same values of $v_2$(0.05, 0.10, 0.20 Hz) were used for Figs. 2 and 3. The value of $v_2$ is given on each theoretical trace. The values of $v_2$ were obtained by calibrating a precision attenuator using an analysis of double resonance spectra obtained with $\mathbf{H}_2$ strong enough to cause large splitting. The experiments described here were restricted to comparatively low values of $v_2$ because larger values produced an appreciable decrease in detector amplification, as monitored by the cyclohexane line.

Besides causing population changes, the strong rf field, $\mathbf{H}_2$, produces a double resonance spectrum which includes new transitions.[1] For the low values of $v_2$ used here, these coherence effects are important only for the directly connected transitions, $B1$ and $B4$. The effects of field inhomogeneity in double resonance are complicated and tend to reduce the inhomogeneity contributions for $B1$ and increase the inhomogeneity contributions for $B4$.[15]

The theoretical traces were computed from Eq. (14) after obtaining H from Eqs. (29) and (34). Uncorrelated external random field was assumed to describe the relaxation.[16] This was a satisfactory description because the sample was not degassed. Within the framework of this model, the relaxation is described by relaxation times $T_A$ and $T_B$ for the hydroxyl and methylene protons, respectively, where

$$T_A^{-1}=\tfrac{2}{3}\gamma_A^2\langle|H_A(t)|^2\rangle_{Av}\tau_c, \qquad (37)$$

with a similar expression for $T_B^{-1}$. In Eq. (37), the expression in angular brackets is the root mean square random field at nucleus $A$, and $\tau_c$ is the correlation time. Therefore, the experimental parameters are $\tau$, $T_A$, $T_B$, and $\lambda$. The value of $\lambda$, the inhomogeneity contribution, was taken to be the half-width at half-height of the cyclohexane resonance, $2\pi$ (0.20) rad/sec. The values of $\tau$, $T_A$, and $T_B$ were determined by visually obtaining the best agreement between the experimental and theoretical traces. The same scale factor was used for all four traces in each figure. This gave $T_A=T_B=8$ sec, and $\tau=4$ sec for Fig. 2; and $T_A=T_B=7$ sec, and $\tau=0.5$ sec for Fig. 3. The theoretical traces were sensitive to variations of about 10% in these numbers.

It is seen that the computed spectra reproduce most of the features observed in the experimental spectra. The main disagreement is for the region around the connected transition $B4$ in Fig. 2. The treatment of field inhomogeneity using the single inhomogeneity parameter $\lambda$ is not adequate for this region. In the computed spectra, the splitting shows up as a line broadening.

From the values of $T_A$ and $T_B$ obtained above, it is seen that the relaxation is substantially the same for Figs. 2 and 3. The differences between the spectra in Figs. 2 and 3 are due to the change in the chemical exchange rate.

Although chemical exchange and relaxation combine in a complicated manner in determining the spectral contours, chemical exchange does produce characteristic features in the observed spectra. Chemical exchange is the only mechanism which can transfer saturation to the antisymmetric line $A2$. The external random field mechanism used here gives zero probability for relaxation transitions connecting levels of different symmetry; however, other relaxation mechanisms will allow these transitions only under exceptional circumstances.[17] It is seen that for a given level of saturation, as measured by the height of $A1$ in the computed spectra, the spread of saturation to the lines not directly connected to $A1$ is enhanced with an increase in chemical exchange rate.

## V. SUMMARY AND CONCLUSIONS

It was shown that the analysis of double spectra of chemically exchanging molecules allows the simultaneous study of chemical exchange and relaxation. Relaxation opposes saturation by driving the spin system towards a Boltzmann distribution, and chemical exchange tends to distribute saturation throughout the spin system. Although relaxation and chemical exchange combine in a complicated manner in determining the spectral contrours, the chemical exchange process does produce characteristic features, such as the spreading of saturation between lines of different symmetry. This was illustrated by double resonance experiments on 2,2,2-trichloroethanol. The relaxation parameters and chemical exchange lifetime were obtained for this self-exchanging system by fitting computed and experimental spectra. This was possible even when the chemical exchange rate was slow compared to the linewidths. The formalism was developed specifically in terms of double resonance eigenfunctions; however, the properties of the exchange coefficients (18)–(22) are valid for an arbitrary basis.

It was found convenient to redefine the unknowns so that the density matrix equations were expressed in terms of a real symmetric matrix. This allowed the solution in terms of an eigenvalue procedure. This procedure allows a more efficient computer computation, and automatically takes into account constraints introduced by the summation relations (6), (20), and (21), and molecular symmetry coupled with the summation relation (22). This automatic feature is useful for computer computations on examples with approximate symmetry because the calculation is guaranteed to be stable.

The eigenvalue procedure is a generalization of similar procedures used for calculations involving either the off-diagonal elements[18] or diagonal elements[19,20] of $\chi$, separately. The obtaining of a symmetric matrix by the construction outlined in Sec. III.D depends on the validity of Relations (7). These relations are always valid for extreme narrowing, and are valid in general if the correlation functions for the long correlation time mechanisms (i.e., scalar coupling to a strongly quadrupolar relaxed nucleus) obey the secular approximation.[21]

## ACKNOWLEDGMENT

The support of this research by the National Science Foundation under Grant GP-11796 is gratefully acknowledged.

## APPENDIX

The formalism will be extended to the exchange of one nucleus between two types of molecules with density matrices $\chi^1$ and $\chi^2$. Equation (11) is then replaced by

$$i\omega_{\alpha\beta}\langle\alpha\mid\chi^1\mid\beta\rangle-\sum_{\alpha'\beta'}R_{\alpha\beta\alpha'\beta'}\langle\alpha'\mid\chi^2\mid\beta'\rangle$$
$$-\sum_{\alpha'\beta'}E_{\alpha\beta\alpha'\beta'}{}^{11}\langle\alpha'\mid\chi^1\mid\beta'\rangle-\sum_{\mu\nu}E_{\alpha\beta\mu\nu}{}^{12}\langle\mu\mid\chi^2\mid\nu\rangle$$
$$=-i2\pi q\omega_{\alpha\beta}\langle\alpha\mid\sum_i v_{0i}\mathfrak{F}_z{}^1(i)\mid\beta\rangle, \quad \text{(A1)}$$

with a similar equation for $\chi^2$. In Eq. (A1), the eigenstates of molecule 1 are labeled by $\alpha$ and $\beta$, and the eigenstates of molecule 2 are labeled by $\mu$ and $\nu$. The exchange coefficients are defined by

$$E_{\alpha\beta\alpha'\beta'}{}^{11}=\tau_1{}^{-1}[(\mathrm{Tr}B^{\alpha\beta}B^{\beta'\alpha'}/N_e)-\delta_{\alpha\alpha'}\delta_{\beta\beta'}], \quad \text{(A2)}$$

$$E_{\mu\nu\mu'\nu'}{}^{22}=\tau_2{}^{-1}[(\mathrm{Tr}B^{\mu\nu}B^{\nu'\mu'}/N_e)-\delta_{\mu\mu'}\delta_{\nu\nu'}], \quad \text{(A3)}$$

and

$$E_{\alpha\beta\mu\nu}{}^{12}=\tau_1{}^{-1}[\mathrm{Tr}B^{\alpha\mu}B^{\nu\beta}/N_n], \quad \text{(A4)}$$

where

$$(B^{\alpha\mu})_{ab}=\sum_f C_{fa}{}^{\alpha}C_{fb}{}^{\mu}, \quad \text{(A5)}$$

with analogous definitions for $B^{\alpha\beta}$ and $B^{\mu\nu}$.

These exchange coefficients have properties analogous to those for the self-exchange case. The coefficients, $E_{\alpha\beta\alpha'\beta'}{}^{11}$, $E_{\mu\nu\mu'\nu'}{}^{22}$, $E_{\alpha\beta\mu\nu}{}^{12}$, and $E_{\mu\nu\alpha\beta}{}^{21}$ all transform according to (18) with respect to a change of basis. In addition, they also satisfy the following properties:

$$E_{\alpha\beta\alpha'\beta'}{}^{11}=E_{\beta\alpha\beta'\alpha'}{}^{11}=E_{\alpha'\beta'\alpha\beta}{}^{11}, \quad \text{(A6)}$$

$$E_{\mu\nu\mu'\nu'}{}^{22}=E_{\nu\mu\nu'\mu'}{}^{22}=E_{\mu'\nu'\mu\nu}{}^{22}, \quad \text{(A7)}$$

$$\tau_1E_{\alpha\beta\mu\nu}{}^{12}=\tau_2E_{\mu\nu\alpha\beta}{}^{21}=\tau_1E_{\beta\alpha\nu\mu}{}^{12}=\tau_2E_{\nu\mu\beta\alpha},{}^{21} \quad \text{(A8)}$$

$$\sum_\alpha E_{\alpha\alpha\alpha'\beta'}{}^{11}=\tau_1{}^{-1}\delta_{\alpha'\beta'}, \quad \text{(A9)}$$

$$\sum_\mu E_{\mu\mu\mu'\nu'}{}^{22}=\tau_2{}^{-1}\delta_{\mu'\nu'}, \quad \text{(A10)}$$

$$\sum_\alpha E_{\alpha\alpha\mu\nu}{}^{12}=\sum_\mu E_{\mu\mu\alpha\beta}{}^{21}=0, \quad \text{(A11)}$$

$$\sum_{\alpha'\beta'}E_{\alpha\beta\alpha'\beta'}{}^{11}\langle\alpha'\mid\sum_i v_{0i}{}^1\mathfrak{F}_z{}^1(i)\mid\beta'\rangle$$
$$+\sum_{\mu\nu}E_{\alpha\beta\mu\nu}{}^{12}\langle\mu\mid\sum_i v_{0i}{}^2\mathfrak{F}_z{}^2(i)\mid\nu\rangle=0. \quad \text{(A12)}$$

Using these relations, one may demonstrate that all of the properties discussed for self-exchange have analogies for heteroexchange. In particular, the steady-state equations may still be expressed as a symmetric array. However, Condition (A8) necessitates one change. Assume that there are $n_1$ unknown elements for $\chi^1$ and $n_2$ unknown elements for $\chi^2$, and that the $n_1\chi^1$ elements are assembled first, and the $n_2\chi^2$ elements are assembled second in the $A$ and $K$ matrices of Eq. (29). Then, to obtain a symmetric array, one must multiply the first $n_1$ rows of $A$ and $K$ by $\tau_1$, and the last $n_2$ rows of $A$ and $K$ by $\tau_2$.

* A preliminary report of this work was presented at the 158th Meeting of the American Chemical Society, New York, N.Y., Sept. 1969.

[1] J. D. Baldeschwieler and E. W. Randall, Chem. Rev. 63, 81 (1962).
[2] (a) B. D. Nageswara Rao, Advan. Magnetic Resonance 4, 271 (1970). (b) All of the symbols used in this paper agree with Refs. 1 and 2(a) except for $v_{ki}$, which differs by a change of sign. This makes $v_{ki}$ a positive quantity for protons.
[3] A. G. Redfield, Advan. Magnetic Resonance 1, 1 (1965).
[4] S. Alexander, J. Chem. Phys. 37, 974 (1962).
[5] R. A. Newmark and C. D. Sederholm, J. Chem. Phys. 43, 602 (1965).
[6] S. Forsen and R. A. Hoffman, J. Chem. Phys. 39, 2892 (1963).
[7] S. Forsen and R. A. Hoffman, J. Chem. Phys. 40, 1189 (1964).

[8] B. M. Fung, J. Chem. Phys. 47, 1409 (1967).
[9] B. M. Fung, J. Chem. Phys. 49, 2973 (1968).
[10] B. D. N. Rao, Phys. Rev. 137, A467 (1965).
[11] C. S. Johnson, Advan. Magnetic Resonance 1, 33 (1965).
[12] A copy of the computer program used for this paper will be supplied upon request. The program is written in FORTRAN V for the UNIVAC 1108.
[13] F. Bloch, Phys. Rev. 102, 104 (1956).
[14] B. D. N. Rao and L. Lessinger, Mol. Phys. 12, 221 (1967).
[15] R. Freeman and W. A. Anderson, J. Chem. Phys. 37, 2053 (1962).
[16] Reference 2, p. 296.
[17] K. F. Kuhlmann and J. D. Baldeschwieler, J. Chem. Phys. 43, 572 (1965).
[18] J. H. Freed and G. K. Fraenkel, J. Chem. Phys. 39, (1963).
[19] J. H. Noggle, J. Chem. Phys. 43, 3304 (1965).
[20] S. L. Gordon, J. Chem. Phys. 48, 2129 (1968).
[21] Reference 2, Eq. (26).

**Erratum: Nuclear Magnetic Double Resonance in Chemically Exchanging Systems**

[ J. Chem. Phys. 54, 1779 (1971) ]

Ping P. Yang and Sidney L. Gordon

School of Chemistry, Georgia Institute of Technology, Atlanta, Georgia 30332

Eqs. (A9), (A10) and (A11) of the appendix should be replaced by the following:

$$\sum_{\alpha} E_{\alpha\alpha\mu\nu}{}^{12} = \tau_1^{-1}\delta_{\mu\nu} , \tag{A9}$$

$$\sum_{\mu} E_{\mu\mu\alpha\beta}{}^{21} = \tau_2^{-1}\delta_{\alpha\beta} , \tag{A10}$$

$$\sum_{\alpha} E_{\alpha\alpha'\beta'}{}^{11} = \sum_{\mu} E_{\mu\mu'\nu'}{}^{22} = 0. \tag{A11}$$

# BIBLIOGRAPHY

1. P. P. Yang and S. L. Gordon, J. Chem. Phys. 54, 1779 (1971).

2. F. Bloch, Phys. Rev. 102, 104 (1956).

3. J. D. Baldeschwiewieler, J. Chem. Phys. 40, 459 (1964).

4. S. L. Gordon, J. Chem. Phys. 45, 1145 (1966).

5. B. D. N. Rao, Phys. Rev. 137, A467 (1965).

6. A. Kumar and S. L. Gordon, J. Chem. Phys. 54, 3207 (1971).

7. R. Freeman and S. Wittekoek, J. Chem. Phys. 52, 1529 (1970).

8. V. Sinivee, Commun. Estonian Acad. Sci. (Phys. Math. Tech. Ser.), 15, 182 (1966).

9. J. H. Noggle, J. Chem. Phys. 43, 3304 (1965).

10. A. Kumar and B.D.N. Rao, Mol. Phys. 15, 377 (1968).

11. S. L. Gordon, J. Chem. Phys. 48, 2129 (1968).

12. R. H. Wakefield and J. D. Memory, J. Chem. Phys. 48, 2174 (1968).

13. F. Bloch, Phys. Rev. 70, 460 (1946).

14. A. Abragam, The Principles of Nuclear Magnetism (Oxford University Press, London, 1961).

15. B. D. N. Rao, Advance in Magnetic Resonance 4, 271 (1970).

16. A. G. Redfield, Advance in Magnetic Resonance 1, 1 (1965).

17. N. R. Krishna, Thesis, Indian Institute of Technology, Kanpur (1971).

18. P. S. Hubbard, Phys. Rev. 131, 1155 (1963).

19. M. E. Rose, Elementary Theory of Angular Momentum (John Wiley & Sons, Inc., New York, 1957).

20. D. W. G. Smith and J. G. Powles, Mol. Phys. 10, 451 (1965/1966).

21. V. S. Watts and J. H. Goldstein, J. Chem. Phys. 42, 278 (1965).

22. C. Manneback and A. Rahman, Ann. Soc. Sci. Bruxelles, Ser. I, 67, 28(1953).

23. W. T. Huntress, Jr., Advance in Magnetic Resonance 4, 1 (1970).

# VITA

The author was born in Taiwan in 1940. After he graduated from high school in his home town, Hu-Wei, he went to Cheng Kung University to study chemical engineering at Tainan. In 1964, he received his B.S. degree in Chemical Engineering. After one year military service in the army he entered the graduate School of Chemistry at Georgia Institute of Technology in 1966. He received his M.S. degree in Chemistry in August 1968. Since then he continued on his Ph.D. work in nuclear spin relaxation mechanisms and enjoyed his research work very much.

He wishes to thank his mother, his brothers (Hayjohn and Tokujohn) and his sister-in-law, Liang-hua for their encouragements.